THE PRODUCTION OF NEGATIVE IONS IN ATOMIC COLLISIONS

Ya. M. FOGEL'

Usp. Fiz. Nauk 71, 243-287 (June, 1960)

I. INTRODUCTION

SINCE the appearance of the second edition of Massey's monograph on negative ions[1] many experimental and theoretical studies have been carried out, which have made a large contribution to this branch of physics.

The increased interest in negative ions that has been manifested in recent years is due to the fact that the elementary processes that lead to the production and destruction of negative ions play a large role in astrophysics and the physics of the upper layers of the atmosphere, in gas discharges and radiation chemistry, and in mass spectrometry and the technology of the acceleration of charged particles.

Negative ions are formed:

a) at the surface of a solid body when it is acted on by a gas or by a molecular or ionic beam (negative surface ionization, secondary negative-ion emission);

b) in collisions of slow electrons with gas molecules;

c) in collisions of ions and atoms with gas molecules.

The results of studies of processes a) and b) have been adequately expounded in a number of monographs and review articles,[2-5] and therefore in the present article we shall consider only processes of negative-ion production in collisions of heavy particles, which have been studied only in quite recent times.

Processes of negative-ion production in atomic collisions can be divided into two classes. The first class includes processes of production of fast negative ions that arise in the passage of fast positive ions or atoms through rarefied gas, as the result of elementary processes in which the fast particle captures one or more electrons from the electronic structure of a gas molecule. Processes of this class can be represented schematically by the formula

$$A^{k+} + B \rightarrow A^- + B^{(k+1)+}. \qquad (I)$$

In this formula A^{k+} represents a fast particle, which may be a positive ion or a neutral atom, depending on the value of $k (0 \leq k \leq z_A)$, and B represents a particle in the gas. Naturally such processes can occur only for particles A that have positive electron affinities.

The second class consists of processes in which slow negative ions are produced. These processes are:

1) charge transfer between negative ions and gas molecules

$$A^- + BC \rightarrow A + BC \begin{cases} \nearrow B^- + C \\ \searrow B + C^- \end{cases}; \qquad (IIa)$$

2) dissociation of a molecule of the gas into positive and negative ions by collision with a fast heavy particle

$$A^{k+} + BC \rightarrow A^{k+} + B^- + C^+ \qquad (-1 < k < Z_A). \qquad (IIb)$$

In spite of their importance to radiation chemistry, processes of the second class have as yet not been studied very much, and therefore the present article will be mainly devoted to processes of the first class. Among the processes of this class, only two have been studied up to the present time, capture of two electrons by a singly charged positive ion (two-electron charge transfer) and capture of one electron by a neutral atom. On the basis of (I), these processes can be represented as follows:

$$A^+ + B \rightarrow A^- + B^{2+} \qquad (k = 1), \qquad (III)$$

$$A + B \rightarrow A^- + B^+ \qquad (k = 0). \qquad (IV)$$

As will be seen from the further exposition, the effective cross sections for processes (III) and (IV) are smaller than the cross sections for other processes of electron capture by positive ions. In particular, they are much smaller than the cross sections found for one-electron capture by singly-charged positive ions (ordinary or one-electron charge transfer), which have been studied in detail. In this connection the question arises as to what considerations can justify the study of these phenomena, which have relatively small probabilities, and what their study can contribute to the physics of atomic collisions. To answer this question it is necessary to give a brief account of the present state of this branch of atomic physics.

One of the main problems in the study of any atomic-collision process is the calculation or experimental determination of the function $\sigma(v)$, that is, the dependence of the effective cross section of the process on the relative velocity of the colliding particles. Theoretical calculations of the effective cross sections of inelastic processes in collisions of heavy particles can be carried out in only a limited number of cases, namely for particles whose electronic structures contain a small number of particles. Even in these cases the calculation is possible either for slow collisions, for which $v \ll v_0$, or for fast collisions, for which $v \gg v_0$ (v is the relative velocity of the colliding particles, and v_0 is the velocity of the electrons in the colliding systems) (cf. reference 6).

The calculation of effective cross sections for electron capture can also be made in those few cases in which the potential energy curves are known for the initial and final states of the colliding particles. In these cases one uses for the calculation of the cross sections a method proposed by L. D. Landau.[7-9] In all other cases some conclusions can be drawn about the curve of $\sigma(v)$ by starting from Massey's adiabatic hypothesis.[10] The basic propositions of this hypothesis are connected with the size of the so-called adiabatic parameter $a|\Delta E|/hv$ (the constant a is the effective distance at which the interaction forces between the colliding particles act,* ΔE is the resonance defect, i.e., the change of the internal energy of the particles as a result of the process, and h is Planck's constant). These propositions are as follows:

1) in the region of small velocities (the adiabatic region), in which the condition $a|\Delta E|/hv \gg 1$ holds, the effective cross sections of inelastic processes are very small and increase with increase of the velocity in accordance with the formula

$$\sigma = \sigma_0 e^{-h\frac{a|\Delta E|}{hv}}; \quad (1)$$

2) the maximum value σ_{max} of an effective cross section is attained at a velocity v_{max} that satisfies the condition

$$\frac{a|\Delta E|}{hv_{max}} \cong 1. \quad (2)$$

After passing through its maximum the effective cross section falls off with further increase of the velocity; consequently, from the point of view of the adiabatic hypothesis the curve of $\sigma(v)$ must be a simple curve with a single maximum.

It has been shown in papers by Hasted and his collaborators[12-17] that Massey's adiabatic hypothesis is entirely applicable to many processes of the capture of one electron by singly charged positive ions. In particular, it has been established that the curves of $\sigma_{10}(v)$† for many ion-molecule combinations are of a simple type, with the position of the maximum given by the adiabatic criterion (2). In cases of one-electron charge transfer in inert gases the quantity a that appears in the criterion (2) changes only slightly as we go from one ion-molecule combination to another, and has an average value of 8 A. The behavior of the cross section $\sigma_{10}(v)$ in the adiabatic region corresponds to Eq. (1). For certain ion-molecule combinations, however, there was obvious lack of agreement of the behavior of the curve of $\sigma_{10}(v)$ with the requirements of the adiabatic hypothesis. This disagreement is of two kinds: 1) the curve of $\sigma_{10}(v)$ has a complicated structure with two, and sometimes even three, maxima; 2) in the low-velocity region $\sigma_{10}(v)$ has anomalously large values. The presence of several maxima in the curve of $\sigma_{10}(v)$ actually does not contradict the adiabatic hypothesis; it is explained by the fact that not only particles in the ground state, but also excited particles, take part in the process being observed. The anomalously large cross sections in the low-velocity region are due to violation of the adiabatic condition $a|\Delta E|/hv \gg 1$ in this region. As Bates and Massey[18] have shown, such a violation can occur when the potential-energy curves of the initial and final states of the system of the colliding particles come so close together at a certain internuclear distance R_M that the minimum difference $\Delta V(R_M)$ of the potential energies is much smaller than ΔE. The character of the potential curves depends on the nature of the colliding particles, and since in the overwhelming majority of cases the potential curves are unknown, the question of the applicability of the adiabatic hypothesis to a given inelastic process can be settled only by experiment.

From what has been said it follows that in the present stage of development of the physics of atomic collisions, when there is no theory that permits us to calculate the effective cross sections of the various processes, it is very important to accumulate new experimental information, on which such a theory may in future be based. It is still very difficult to say what sort of experimental studies will be most useful for the construction of a future theory of atomic collisions, but we can try to formulate some general propositions.

First of all, it is desirable to study as many different processes of atomic collision as possible, since comparisons of the properties of different processes can be extremely instructive. It is also very important to examine the applicability of the adiabatic hypothesis to each process that is studied. Studies must be made on both the total cross sections of the various processes, and also on the differential scattering cross sections. Other points of great interest are the energy loss of the fast particle, and the distributions in angle and energy of the slow particles produced in the collision. We believe it is also desirable to study processes in which the shape of the curve of $\sigma(v)$ for the process in question is not distorted by the presence of excited particles in the initial state or by their production in the final state. It must also be noted that processes with small cross sections may turn out to be of interest for the theory, and also processes that are accompanied by weak scattering.

We can indicate the following features of processes (III) and (IV) that justify an interest in studying them.

1) These processes have not been studied earlier.

2) In the case of process (III) for certain ion-molecule combinations (H^+ in H_2 and He, alkali-metal ions from thermionic sources in H_2 and He) the curve obtained for $\sigma(v)$ is not distorted by the occurrence of particles in an excited state. The shape of such a "pure" curve can be of great interest for the theory of atomic collisions.

*A different interpretation of the quantity a that appears in the adiabatic parameter is given in reference 11.

†σ_{ik} is the effective cross section of a process in which a particle of charge ie is converted into a particle with charge ke.

3) In the case in which all of the particles involved in the process are in their ground states, the resonance defect of process (III) is calculated from the formula

$$\Delta E_0 = (S_A + V_A^I) - (V_B^I + V_B^{II}), \quad (3)$$

where S_A and V_A^I are the electron affinity and first ionization potential of particle A, and V_B^I and V_B^{II} are the first and second ionization potentials of particle B. It follows from Eq. (3) that ΔE_0 is always negative (the process is endothermal) and is large, in many cases amounting to some tens of ev. The large value of ΔE_0 for process (III) makes it improbable that the potential curves of the initial and final states of the system will come close together at the internuclear distances that are attained at energies of the order of tens of kev, so that there is a possibility of applying the adiabatic hypothesis to the process $A^+ \rightarrow A^-$. On the other hand, the large value of ΔE_0 facilitates the study of the adiabatic region, which is defined in terms of the quantity $a|\Delta E|/hv$, since for large values of ΔE this region corresponds to larger velocities of the primary beam than is the case, for example, for one-electron charge transfer, for which ΔE is in most cases small.

4) Process (IV) is interesting because here, unlike the cases of capture of electrons by singly and multiply charged positive ions, the electron is captured to an electron-affinity level with a small binding energy.

We must also point out that the study of processes (III) and (IV) is of practical interest from the point of view of developing sources of negative ions for electrostatic accelerators of the charge-transfer type.[19] In these sources use is made of the conversion of positive ions into negative ions in the passage of an ion beam through matter, in which processes (II) and (IV) play an extremely important role.

The present article gives a description of the apparatus and methods used to measure effective cross sections for the production of negative ions in atomic collisions, a discussion of the results of measurements of the cross sections for processes (III) and (IV), and an examination of the following questions:

a) the dependence of the shape of the curve of $\sigma(v)$ on the nature of the pair of colliding particles;

b) the interpretation of the shape of the curve of $\sigma(v)$ on the basis of the Massey adiabatic hypothesis, with the occurrence of excited particles in the process taken into account;

c) the behavior of the curve of $\sigma(v)$ in the low-velocity region ($a|\Delta E|/hv \gg 1$);

d) the behavior of the curve of $\sigma(v)$ in the region $v > v_{max}$;

e) the dependence of the maximum cross section on various factors;

f) comparisons of the cross sections of various electron-capture processes.

Some data on the production of slow negative ions in atomic collisions are presented at the end of the article.

II. APPARATUS AND METHODS USED FOR THE MEASUREMENTS

The methods of Wien,[20] based on the weakening of the beam and the collection of slow ions at a measuring electrode, are not applicable to measurements of the cross sections σ_{1-1} and σ_{0-1} of processes (III) and (IV); these methods have been widely used earlier (and are also used at present), and have been discussed in detail in the survey article by Allison.[21] We can easily convince ourselves that these methods cannot be used by considering the example of the simplest processes $H^+ \rightarrow H^-$ and $H^0 \rightarrow H^-$. The beam produced by the passage of H^+ or H^0 particles through matter is a three-component system, containing hydrogen in three charge states (H^+, H^0, and H^-), and the Wien method is useful only for determining the cross sections σ_{10} and σ_{01} in the two-component system of H^+ and H^0. For an H^+ beam the method of the weakening of the beam gives the sum of the cross sections $\sigma_{10} + \sigma_{1-1}$, and for a H^0 beam it gives the sum $\sigma_{01} + \sigma_{0-1}$. The method of collection of slow ions at a measuring electrode, together with mass-spectrometric analysis of the composition of the slow ions, gives the sum of the cross sections $\sigma_{1-1} + \sigma_{02}^i$ (σ_{02}^i is the cross section for ionization with removal of two electrons from a gas molecule of the target).

The measurement of the cross sections σ_{1-1} and σ_{0-1} has been carried out by means of a mass-spectrometric method which was first applied by Korsunskiĭ and his co-workers[22] to measure the cross sections for electron loss by Li^+ and Na^+ ions, and later was further developed simultaneously and independently by Ya. M. Fogel' and his co-workers[23-28] and by V. M. Dukel'skiĭ and N. V. Fedorenko.[29,30]

The main point of the mass-spectrometric method can be most simply illustrated by the example of the three component system that arises from the passage of protons through matter. The composition of such a beam is described by the differential equations

$$\frac{dN^+}{d(nx)} = -(\sigma_{10} + \sigma_{1-1})N^+ + \sigma_{01}N^0 + \sigma_{-11}N^-, \quad (4a)$$

$$\frac{dN^0}{d(nx)} = \sigma_{10}N^+ - (\sigma_{01} + \sigma_{0-1})N^0 + \sigma_{-10}N^-, \quad (4b)$$

$$\frac{dN^-}{d(nx)} = \sigma_{1-1}N^+ + \sigma_{0-1}N^0 - (\sigma_{-11} + \sigma_{-10})N^-, \quad (4c)$$

where N^+, N^0, and N^- are the numbers of protons, neutral hydrogen atoms, and negative hydrogen ions in the beam, n is the number of target gas atoms per cubic centimeter, and x is the path length in the gas.

By using the initial conditions $nx = 0$, $N^+ = N_0^+$, $N^0 = 0$, $N^- = 0$ one easily gets from Eq. (4c) the following formula for the determination of the effective cross section for capture of two electrons by a proton:

$$\sigma_{1-1} = 1.08 \cdot 10^{-19}\left(\frac{T}{L}\right)\left[\frac{d\left(\frac{I^-}{I_0^+}\right)}{dp}\right]_{p=0}, \quad (5)$$

where L is the effective length of the collision chamber, T and p are the temperature and pressure of the gas in the collision chamber, I^- is the current of negative hydrogen ions in the emerging beam, and I_0 is the current of the proton beam entering the collision chamber.

The method for measuring the cross section σ_{1-1} that follows from Eq. (5) consists in studying the dependence of the ratio I^-/I_0 on the pressure p of the gas in the collision chamber. From the linear part of the curve, which is due to the production of negative ions in single collisions of protons with gas molecules, one determines the derivative that appears in Eq. (5), and then calculates the desired cross section from Eq. (5).

In order to satisfy the condition that the main process is that of single collisions, it is necessary in some cases to study the dependence on the gas pressure at very low pressures. It is possible, however, to determine the cross section also in cases in which the condition of single collisions is not satisfied. To do this one must use the solutions of the differential equations (4), which are:

$$\left.\begin{aligned} N^+ &= a_0 + a_1 e^{-r_1 nx} + a_2 e^{-r_2 nx}, \\ N^0 &= b_0 + b_1 e^{-r_1 nx} + b_2 e^{-r_2 nx}, \\ N^- &= c_0 + c_1 e^{-r_1 nx} + c_2 e^{-r_2 nx}, \end{aligned}\right\} \qquad (6)$$

where the quantities r_1, r_2, a_0, a_1, and so on are functions of the six cross sections that appear in the differential equations (4). For sufficiently small values of $r_1 nx$ and $r_2 nx$ the expressions (6) for N^+ and N^- can be expanded in series. Dividing N^- by N^+ and neglecting powers of nx higher than the second, we get:

$$\frac{I^-}{I^+} = \sigma_{1-1} nx + \frac{1}{2}(\sigma_{10}\sigma_{0-1} + \sigma_{1-1}\sigma_{10} + \sigma_{1-1}^2 - \sigma_{1-1}\sigma_{-10} - \sigma_{1-1}\sigma_{-11})(nx)^2. \qquad (7)$$

Thus, in a range of gas pressures in the collision chamber in which, on one hand, multiple collisions of beam particles with gas molecules are beginning to be important, and, on the other hand, the pressure is still not very large, the dependence of the ratio I^-/I^+ on the pressure is given by the formula

$$\frac{I^-}{I^+} = \gamma p + \delta p^2, \qquad (8)$$

where

$$\gamma = \sigma_{1-1}\frac{L}{kT},$$

$$\delta = \frac{1}{2}(\sigma_{10}\sigma_{0-1} + \sigma_{1-1}\sigma_{10} + \sigma_{1-1}^2 - \sigma_{1-1}\sigma_{-10} - \sigma_{1-1}\sigma_{-11})(nx)^2. \qquad (9)$$

By treating the experimental data by the method of least squares one can determine the coefficient γ of the linear term in Eq. (8), and thus calculate the cross section σ_{1-1}.

A set of points that satisfy Eq. (8) can be picked out by plotting the expression $(I^-/I^+)/p$ against p. It is easy to see that the points that fall on the straight-line part of the plot satisfy Eq. (8).

The presence or absence of a linear section in the curve of $I^-/I^+ = f(p)$ in this range of pressures is determined by the value of the quantity $(\delta/\gamma)p$. If the condition $(\delta/\gamma)p \ll 1$ is not satisfied in any part of the pressure range in question, there will be no linear part. If this condition is satisfied over the entire range, the dependence of I^-/I^+ on p is linear.

The method for determining the cross section σ_{1-1} remains the same for singly charged ions more complicated than the proton. The only difference is that the beam that has passed through the gas is not a three-component system, since in addition to singly charged positive ions, neutral atoms, and negative ions the beam can contain also doubly charged ions, triply charged ions, and so on, which have arisen owing to processes in which particles of the primary beam lose electrons in collisions with the gas molecules. In this case there is an increase both in the number of terms in each equation of the system (4) and in the number of the equations themselves, so that both are equal to the number of charge states in the beam emerging from the matter. The formula (5) for calculating the cross section σ_{1-1} remains valid, however, and so does the expression (8) for the ratio I^-/I^+; the only difference is that the coefficient δ in Eq. (8) is a function of a larger number of cross sections.

A great advantage of the mass-spectrometric method is that it can be used to measure the cross section σ_{ik} of any process, in which a particle of the primary beam with charge ie is converted into a particle with the charge ke. The difference in the experimental conditions in the determination of these cross sections is that when one is determining the cross section σ_{0-1} a beam of neutral atoms enters the collision chamber, and one determines the dependence of the ratio N^-/N^0 in the emerging beam on the pressure in the collision chamber.

As can be seen from the foregoing discussion of the mass-spectrometric method, the experimental apparatus with which one can measure by this method the effective cross sections of processes accompanied by changes of the charge state of fast particles must consist of the following main units: 1) a system that produces a monoenergetic beam of primary particles, homogeneous in composition and directed into the collision chamber, 2) a collision chamber, which is a penetrable gaseous target of thickness nx which can be varied and measured with suitable accuracy, and 3) a system that produces a separation of the beam emerging from the collision chamber into components with different charge states and provides measurements of the intensities of the various components.

A diagram of the apparatus used to measure the cross sections σ_{1-1} and σ_{0-1} is shown in Fig. 1. The beam of singly charged positive ions is produced by an ion gun consisting of the high-frequency ion source 1, the

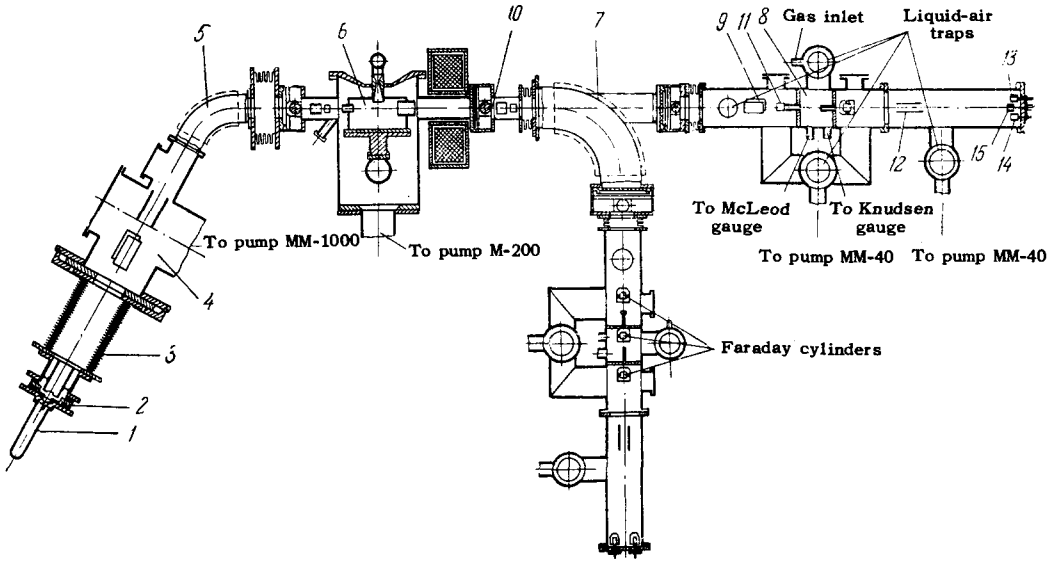

FIG. 1

three-electrode lens 2, and the accelerating tube 3. The ion beam can be shifted and turned by means of a flat ground joint and the electrostatic corrector 4. The magnetic mass-monochromator 5 separates from the ion beam a component that is monoenergetic and homogeneous in its value of m/e and directs it into the mercury-vapor target chamber 6. The mercury-vapor target is an ultrasonic stream of mercury vapor moving in vacuum. A detailed description of the mercury-vapor target is contained in references 31 and 32, so that we shall not consider it further here. As a result of captures and losses of electrons in collisions of ions of the beam with mercury atoms in the target stream, the emerging beam contains, in addition to particles that have retained their original charge state, also particles in other charge states, in particular neutral atoms and negative ions. A second magnetic analyzer 7 separates the charged particles from the neutral ones. The beam of neutral particles, after being collimated by two diaphragms 10 and 11 (of diameters 3 and 2 mm, respectively) was sent into the collision chamber 8. Charged particles are present in the atomic beam as a small impurity, owing to collisions of atoms of the beam with residual gas molecules on the way from the magnetic analyzer 7 to the entrance diaphragm of the collision chamber 8. To remove these charged particles from the neutral beam that enters the collision chamber, a parallel-plate capacitor 9 was placed in front of the entrance to the chamber. The beam entered and left the collision chamber through channels of diameter 5 mm and length 50 mm. The distance from the exit plane of the entrance channel to the entrance plane of the exit channel was 50 mm.

The separation of the beam emerging from the collision chamber into neutral, positive, and negative components was made by an electric field in the parallel-plate capacitor 12. The currents of the charged components were measured by means of the Faraday cylinders 13 and 14, which were connected to EMU-3 vacuum-tube electrometer of maximum sensitivity 10^{-14} amp/div. Absolute measurements of the intensity of the neutral beam were made by means of the vacuum thermal element 15, which was connected to a M107/3 mirror galvanometer of sensitivity 2×10^{-8} v/div. The construction of this thermal element and the method of working with it are described in references 27 and 33.

A second collision chamber, with its axis perpendicular to that of the first chamber, was provided for the study of processes of electron capture and electron loss by positive and negative ions. Its construction and dimensions are the same as those of the first chamber. To produce beams of protons and He^+ ions, hydrogen and helium were admitted to the source bulb; for C^+ and O^+ ions, carbon dioxide; for B^+ and F^+ ions, BF_3; for Cl^+ ions, CCl_2F_2; and for Li^+, Na^+, and K^+ ions, vapors of LiCl, NaCl, and KCl. In the apparatus described in reference 34, the ions Li^+, Na^+, and K^+ were obtained from a thermionic source, which was a tungsten helix coated with aluminosilicates of Li, Na, and K.

In measurements of the cross section σ_{1-1} by the mass-spectrometric method there are a number of sources of systematic errors. These sources are as follows:

a) Contamination of the Primary Beam by Ions of Different Nature, but with the Same Mass and Charge

The only case of this sort in the experiments to be described here was the possible contamination of the beam of F^+ ions by H_3O^+ ions, which could be formed in the plasma of the ion source by the ionic-molecular reaction $H_2O^+ + H_2O \rightarrow H_3O^+ + OH$.[35] No H_2O^+ ions were observed, however, in the mass spectrum of the high-frequency discharge in BF_3. On the other hand, a study of the mass spectrum of the ions obtained from a high-frequency discharge in water vapor showed that the intensity of the beam of H_3O^+ ions was smaller

than that of the beam of H_2O^+ ions by about a factor of 7 or 8. Besides this, measurements of the cross section σ_{1-1} for H_3O^+ ions in Ar at 30 kev showed that it was two orders of magnitude smaller than the cross section σ_{1-1} for F^+ ions under the same conditions. All of this allows us to conclude that the results of the measurements of the effective cross section σ_{1-1} for F^+ cannot be affected by the presence of H_3O^+ ions as an impurity in the beam.

b) Fragment Ions as Impurities Added to the Primary Beam

In cases in which complex chemical compounds are used as the working substance in the ion source, there is the possibility of contamination of the primary beam by fragment ions due to dissociation of heavier molecular ions in the space between the ion source and the mass monochromator. Such contamination is possible when the apparent mass m^* of a fragment ion is close to the mass of the ions of the primary beam ($m^* = m_1^2/M$, where m_1 is the mass of the fragment ion and M is the mass of the molecular ion before dissociation). Such contamination was possible in only one case, namely when Cl_{35}^+ ions were obtained from a discharge in CCl_2F_2. An apparent mass close to 35 can be shown by ClF^+ and CCl^+ ions that arise from the dissociation of $CClF_2^+$ and $CClF^+$ ions. To verify the absence of these ions in the beam of Cl^+ ions, this beam was sent through the collision chamber, and the emerging beam was analyzed with an electrostatic analyzer. Since the electrostatic analyzer separates the ions according to their energies, the ClF^+ and CCl^+ ions, having smaller energies than the Cl^+ ions, must be separated from them. These ions were not found in the energy spectrum of the beam of mass 35. Thus the value of the cross section of the process $Cl^+ \rightarrow Cl^-$ could not have been falsified by the presence of fragment ions. This conclusion is further confirmed by control measurements of the cross section σ_{1-1} made with Cl^+ ions obtained from a discharge in CCl_4 vapor. In this case contamination of the primary beam by fragment ions is impossible, and the value obtained for the cross section σ_{1-1} was the same as with the Cl^+ beam obtained from the discharge in CCl_2F_2.

c) Neutral Atoms as Impurities in the Primary Beam of Positive Ions

The primary beam always contains some neutral atoms which have been produced by neutralization of ions at the entrance diaphragm of the collision chamber, and also in collisions of ions with residual gas molecules on their way from the mass monochromator to the entrance diaphragm. If the concentration of neutral atoms in the primary beam is K, then the measured cross section will be larger than the true value by the factor $[1 + K(\sigma_{0-1}/\sigma_{1-1})]$, i.e., the systematic error caused by an admixture of neutral atoms will be small if $K(\sigma_{0-1}/\sigma_{1-1}) \ll 1$.

In order to diminish this error, a liquid-nitrogen trap is placed in the space between the mass monochromator and the collision chamber, to lower the pressure of the residual gas in this space; besides this, entrance diaphragms with sharp edges are used.

In addition to these measures, control experiments were made to find out the magnitude of the systematic error in question. In these experiments a parallel plate capacitor placed immediately after the enterance channel of the collision chamber was used to produce a transverse electric field which removed the charged components from the beam entering the chamber. The neutral atoms mixed with the beam passed through the chamber, and those that captured one electron from gas molecules were converted into negative ions. The amount I_1^- of these negative ions can be compared with the total amount I_0^- of negative ions produced with the same pressure in the collision chamber in the case in which the entire primary beam is admitted to the collision chamber (the capacitor plates are grounded). The ratio I_1^-/I_0^- at once gives the size of the systematic error under consideration. For the majority of the ion-molecule combinations that have been studied the size of this error does not exceed 10 percent; it reached 14 percent only for the combination $C^+ - Kr$ at energy 50 kev. Thus the neutral-atom impurity in the primary beam has only a small effect on the results of the measurements. In the apparatus devised for the measurement of the very small cross sections of two-electron charge transfer to alkali-metal ions, the neutral-atom impurity in the primary beam is eliminated by placing a parallel-plate capacitor between the entrance diaphragm and the entrance channel of the collision chamber.

d) Neutralization of Positive and Negative Ions at the Entrance Diaphragm of the Analyzer and in the Analyzer Chamber

The formula (8) for the determination of the value of the cross section σ_{1-1} contains the values I^- and I^+ of the negative-ion and positive-ion currents right at the exit from the collision chamber. But the values of the currents I^- and I^+ actually measured by the Faraday cylinders of the analyzer must be somewhat diminished because of neutralization of ions, both at the diaphragm of the exit channel of the collision chamber and in collisions with residual-gas molecules in the analyzer chamber.

Comparison of the values of I_1^-/I_0^- with the data from measurements of the cross section σ_{0-1} enables us to estimate the number of atoms that appear owing to neutralization of positive ions at the edges of the diaphragm. Estimates made in this way for the ions H^+, C^+, and O^+ give for the fraction of neutral ions the values 0.1, 2.5, and 3 percent, respectively. The neutralization of the negative ions at the edges of the diaphragm cannot be much larger. As for the neutralization of positive and negative ions by residual gas mole-

cules in the analyzer chamber, it was found that freezing out of the vapors in the analyzer chamber that were condensable at the temperature of liquid nitrogen (i. e., reducing the residual gas pressure in the analyzer chamber to a fraction of its former value) had no effect on the value of σ_{1-1}.

e) Production of Negative Ions by Collisions with Residual Gas Molecules in the Collision Chamber

In measurements of σ_{1-1} by the mass-spectrometric method, one must take into account the fact that some of the negative ions in the emerging beam have been produced in collisions with the residual gas in the collision chamber. This is done by determining the cross section σ_{1-1} from a curve of $(I^-/I^+) - (I^-/I^+)_B = f(p - p_B)$, where $(I^-/I^+)_B$ is the value of the ratio I^-/I^+ for a beam that has passed through the residual gas in the collision chamber, and p_B is the pressure of the residual gas. It is easy to show that this way of taking the effect of the residual gas ("background") into account leads to correct results only when the difference $(I^-/I^+) - (I^-/I^+)_B$ depends linearly on $p - p_B$ in the range of pressures in question. If the dependence is parabolic, a simple calculation shows that the measured cross section σ_{1-1} can be expressed in the following form:

$$\sigma_{1-1\,\mathrm{meas}} = \sigma_{1-1\,\mathrm{true}} + \frac{1}{2}\left[\sigma_{1-1}\sum_{i=1}^{N}(\sigma_{10}^{i}+\sigma_{1-1}^{i})\,p_i + (\sigma_{10}+\sigma_{1-1})\sum_{i=1}^{N}\sigma_{1-1}^{i}\,p_i\right]\frac{L}{kT}, \qquad (10)$$

where p, σ_{10}, σ_{1-1} are the pressure and the cross sections for capture of one and two electrons for the gas in question, and p_i, σ_{10}^{i}, and σ_{1-1}^{i} are the corresponding quantities for one of the gases which make up the residual gas in the collision chamber.

The presence of the second term in Eq. (10) shows that owing to the presence of residual gas in the collision chamber the measured value of the cross section σ_{1-1} is larger than the true value. Because of this fact the presence of condensable vapors in the residual gas in the chamber has an important effect on the value of the measured cross section. If the vapors of organic substances in the collision chamber are condensed on a liquid-nitrogen trap, the residual gas pressure is decidedly lowered, and thus this systematic error is decreased.

For all the ion-molecule combinations that were studied it was established experimentally that further decrease of the quantity $(I^-/I^+)_B$, as compared with its value when the condensable vapors are frozen out, does not lead to a decrease of the measured value of σ_{1-1}. This means that when the condensable vapors in the collision chamber are frozen out the systematic error associated with the presence in the collision chamber of gases that cannot be condensed at liquid-nitrogen temperature is small.

f) Dissimilar Scattering of Primary and Secondary Particles in the Gas in the Collision Chamber

As has been pointed out earlier, in order to obtain the necessary pressure differential the collision chamber is separated from the space in which the emerging beam is analyzed by a channel. The presence of this channel has the consequence that a primary or secondary particle that has undergone scattering at some point of its path in the collision chamber can fail to emerge from it if the angle of scattering is larger than the maximum angle of emergence of a particle from the chamber, which is fixed by the distance of the point where the scattering occurs from the exit plane of the channel and by the diameter of the channel.

Primary particles either undergo elastic scattering or are scattered in inelastic processes in which the charge of the primary particle is not changed (excitation or ionization of an atom of the gas by impact of the primary particle); as for the secondary particles, they are scattered in the very process of their production, and can also be scattered elastically in a second collision.

The dependence of the differential scattering cross section on the angle of scattering can be different for different processes,[36] and this can bring about an error in the measurement of the ratio N^-/N^+. The quantity that can actually be measured is N^{-1}/N^{+1}, which is connected with the quantity N^-/N^+ by the relation

$$\frac{N^{-1}}{N^{+1}} = \frac{C_1}{C_2}\frac{N^-}{N^+}, \qquad (11)$$

where the constants C_1 and C_2 appear as measures of the proportions of the primary and secondary particles that emerge through the channel from the collision chamber. It is easy to see that the equation $N^{-1}/N^{+1} = N^-/N^+$ is correct in two cases: 1) $C_1 = C_2 = 1$, i. e., all the primary and secondary particles emerge through the channel from the collision chamber, and 2) $C_1 = C_2 = 1$, i. e., the primary and secondary particles are scattered in the same way. If neither of these conditions is satisfied, the scattering of the particles in the collision chamber leads to a systematic error in measurements of effective cross sections by means of the mass-spectrometric method.

This error can be estimated by calculation if the dependences of the differential cross section for scattering into unit solid angle on the angle of deflection in the center-of-mass system are known for the various collision processes that are accompanied by scattering of primary or secondary particles. Since these cross sections are unknown for the process in question, such a calculation is impossible.

An experimental estimate of the degree to which the dissimilar scattering of the primary and secondary particles affects the measured value of the cross section was obtained in the following way. The mean solid angle for emergence of particles from the collision chamber was varied by stopping down the exit channel with diaphragms, and the cross section was measured

at various values of this mean solid angle. It is obvious that if dissimilar scattering of the particles is affecting the measured value of the cross section, then this measured value will be found to depend on the mean solid angle of emergence of the particles from the collision chamber, and that as this angle is increased the measured cross section must approach the true value. If, on the other hand, there is no such effect, the measured cross section will not depend on the mean solid angle of emergence of particles from the collision chamber. Experiments of this sort were carried out with ions and atoms, and in all cases showed that there was no dependence of the measured cross section on the mean solid angle of emergence of particles from the collision chamber. It could be concluded from these experiments that in the cases investigated the primary and secondary particles were scattered through angles that did not exceed 1°, and therefore their scattering does not affect the measured value of the cross section. This conclusion has been confirmed by measurements of the cross section σ_{1-1} by a different method,[28] in which the effect of the dissimilar scattering on the measured value of the cross section is incomparably smaller than in the mass-spectrometric method.

The systematic errors that have been considered occur also in measurements of the cross section σ_{0-1}. An analysis similar to that which we have described has shown that these errors cannot seriously alter the results of measurements of the cross section σ_{0-1}.

For each energy of the particles the values of the cross sections were obtained from the average of two measurements. In the vicinity of the maximum of the curve of $\sigma(E)$ five or six measurements were made for each energy value. The magnitude of the random error calculated for an individual measurement depended on the ratio

$$\frac{I^-/I^+ - (I^-/I^+)_B}{(I^-/I^+)_B}$$

for cross sections $10^{-16} - 10^{-17}$ cm^2 it was about ± 7 percent, and for cross sections of 10^{-18} cm^2 and smaller it was ± 30 percent. For the cross sections obtained by averaging a large number of measurements, the statistical error did not exceed ± 3 percent. The error in the measurement of the energy of the particles was ± 3 percent.

III. THE RESULTS OF THE MEASUREMENTS

The process $A^+ \rightarrow A^-$ was studied for 59 ion-molecule combinations, and the process $A^0 \rightarrow A^-$ for 39 atom-molecule combinations. For the former process curves of $\sigma(v)$ were obtained mainly in the range 5-60 kev, and for the latter process, in the range 10-60 kev. The combinations studied are indicated in Table I. The results of these investigations have been presented in references 25 — 27, 34, 37 — 44.

Out of the 19 ions from H^+ to K^+, process III was studied for 9 ions, mainly those of atoms of the second row of the periodic table. The ions Be^+, Mg^+, Ne^+, and Ar^+ were not studied, since the corresponding atoms do not form negative ions. Although the N^- ion exists, the cross section for the process $N^+ \rightarrow N^-$ is very small,[40] and therefore this process was not studied in detail. The ions Al^+, Si^+; P^+, and S^+ remained uninvestigated. The rather wide range of masses of the ions that were studied allowed the hope that for the lightest ions it would be possible to study the velocity range $v > v_{max}$, and for the heavy ions, the adiabatic region. Besides this, it was supposed that for a number of the ion-molecule combinations that were studied the maximum of the cross section would be in the range of velocities accessible to the measurements. As will be seen below, these expectations were justified. It must also be pointed out that the ions that were studied have different structures in their electron shells and differ markedly in their energies of neutralization, and that the corresponding atoms have very different values of electron affinity.

In view of the fact that the treatment of the results is simpler for monatomic target gases, the process was studied in five inert gases. Among the molecular gases hydrogen is of the greatest interest, since two-electron charge transfer in hydrogen leads to the production of two slow protons, i. e., particles that cannot

TABLE I

$A^+ \rightarrow A^-$		$A^0 \rightarrow A^-$	
Gas	Ion	Gas	Atom
Helium . . .	H^+, He^+, Li^+, C^+, O^+, F^+	Helium . . .	H, He, B, C, O, F
Neon . . .	H^+, He^+, Li^+, C^+, O^+, F^+	Neon . . .	H, He, B, C, O, F
Argon . . .	H^+, He^+, Li^+, C^+, O^+, F^+, Na^+, Cl^+, K^+	Argon . . .	H, He, B, C, O, F
Krypton . . .	H^+, He^+, Li^+, B^+, C^+, O^+, F^+, Na^+, Cl^+, K^+	Krypton . . .	H, He, B, C, O, F
Xenon . .	H^+, Li^+, B^+, C^+, O^+, F^+, Na^+, Cl^+, K^+	Xenon . . .	H, He, B, C, O, F
Hydrogen . .	H^+, Li^+, B^+, C^+, O^+, F^+, Na^+, Cl^+, K^+	Hydrogen . .	H, C, O
Nitrogen . .	H^+, Li^+, C^+, O^+, Cl^+	Nitrogen . .	H, C, O
Oxygen . .	H^+, Li^+, C^+, O^+, Cl^+	Oxygen . .	H, C, O

be in excited states. For some ions process (III) was studied in nitrogen and oxygen.

Apart from the foregoing considerations, the choice of the atoms for which process (IV) was studied was determined by the fact that the electron affinity increases monotonically through the list of atoms chosen, He, B, H, C, O, and F.

a) Dependence of the Shape of the Curve of $\sigma(v)$ on the Choice of the Pair of Colliding Particles

Process $A^+ \rightarrow A^-$

The shape of the curve of $\sigma_{1-1}(v)$ depends strongly on the nature of the members of the pair of colliding particles.

Differences in the shapes of the curves of $\sigma_{1-1}(v)$ are also due to the fact that the range of velocities studied is different for ions of different masses. The simplest shape of the curve of $\sigma_{1-1}(v)$, with one rather narrow symmetrical maximum, is obtained for the combinations $H^+ - H_2$, $H^+ - He$, and $Li^+ - H_2$ (Fig. 2), for which particles in excited states cannot participate in the process of two-electron charge transfer. For the process $H^+ \rightarrow H^-$ in Ne, Ar, Kr, and Xe the curves of $\sigma_{1-1}(v)$ (Fig. 3) show more complicated shapes than the corresponding curve for He. In Ne the curve is asymmetrical; on the high-velocity side the fall is less steep than on the low-velocity side. The curves for Ar, Kr, and Xe have two maxima — a narrow one at a lower velocity and a wider one at a higher velocity. The curves of $\sigma_{1-1}(v)$ for the process $F^+ \rightarrow F^-$ in Ne, Ar, Kr, and Xe (Fig. 4) have a complicated structure with two maxima.* Curves with two maxima are also obtained for $F^+ \rightarrow F^-$ in H_2 and for $O^+ \rightarrow O^-$ in Xe.

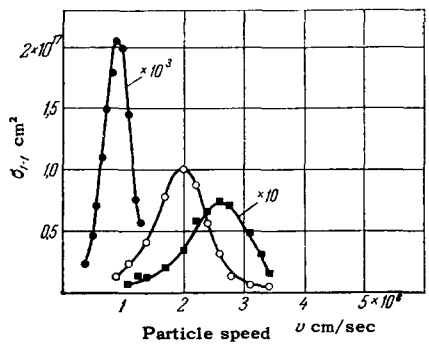

FIG. 2. ● – Li – H_2, ○ – H^+ – H_2, ■ – H^+ – He.

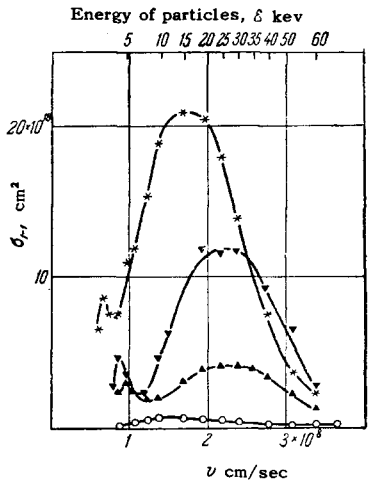

FIG. 3. ○ – Ne, ▲ – Ar, ▼ – Kr, * – Xe.

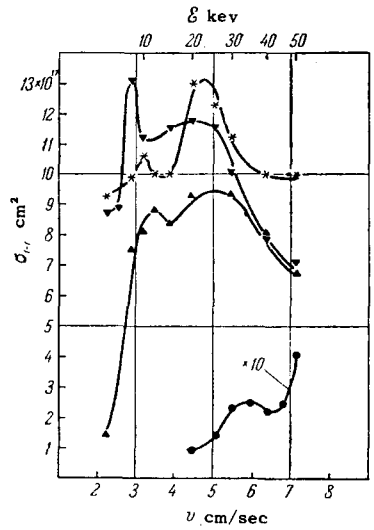

FIG. 4. ● – Ne, ▲ – Ar, ▼ – Kr, * – Xe ($v \times 10^7$ cm/sec).

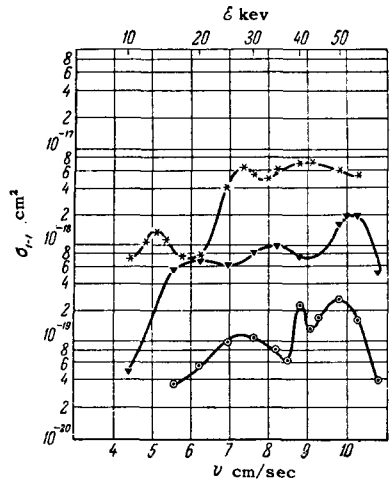

FIG. 5. ⊙ – H_2, ▼ – Kr, * – Xe ($v \times 10^7$ cm/sec).

The curves for the process $B^+ \rightarrow B^-$ in Kr, Xe, and H_2 have a still more complicated structure with three maxima.

In cases in which a maximum of the cross section corresponds to a velocity larger than any in the range of velocities investigated, the curve of σ_{1-1} rises monotonically and rapidly with increasing velocity. This is the situation for the process $Na^+ \rightarrow Na^-$ in Ar, Kr, Xe, and H_2 (curve for thermionic source in Fig. 6).

Process $A^0 \rightarrow A^-$

For the process $A^0 \rightarrow A^-$ one finds mainly curves of $\sigma_{0-1}(v)$ of simple shape with one maximum. As an

*Although the second maximum of the curve of σ_{1-1} for Ne has not been definitely located, the shape of the curve shows that it must exist.

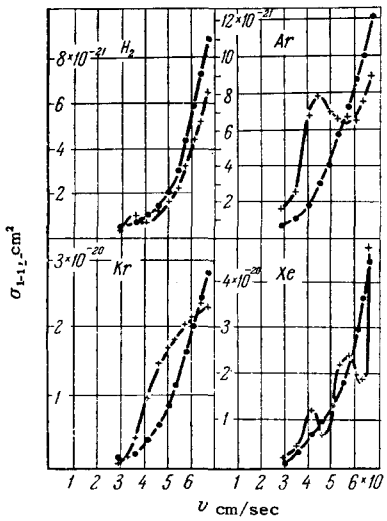

FIG. 6. The process $Na^+ \rightarrow Na^-$. –●– thermionic source; –+–, high-frequency source.

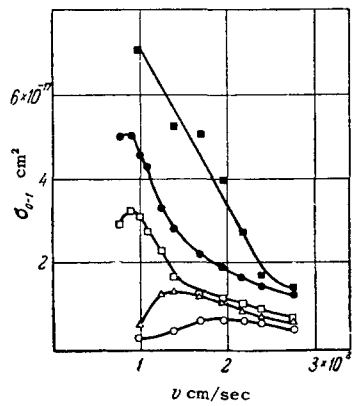

FIG. 7. o – He, Δ – Ne, □ – Ar, ● – Kr, ■ – Xe.

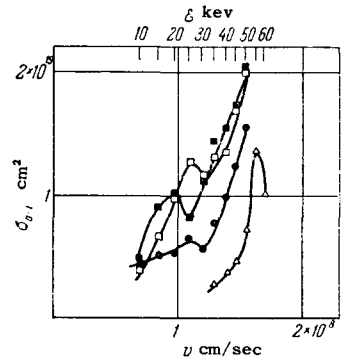

FIG. 8. Δ – Ne, □ – Ar, ● – Kr, ■ – Xe.

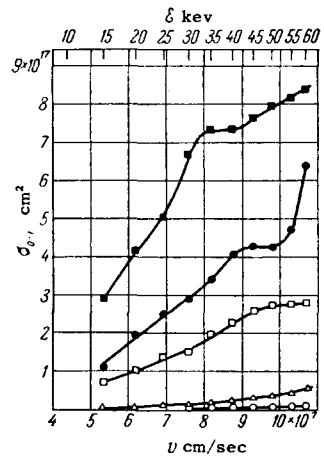

FIG. 9. o – He, Δ – Ne, □ – Ar, ● – Kr, ■ – Xe.

example we show in Fig. 7 the curves of $\sigma_{0-1}(v)$ for the process $H^0 \rightarrow H^-$ in He, Ne, Ar, Kr, and Xe. A more complicated shape is shown by the curves for the process $He^0 \rightarrow He^-$ in Ar, Kr, and Xe (Fig. 8) and the process $B^0 \rightarrow B^-$ in Kr, and Xe (Fig. 9). The behavior of these curves indicates the presence of second maxima at velocities higher than the largest velocities in the range investigated.

b) Interpretation of the Shape of the Curve of $\sigma(v)$ on the Basis of the Massey Adiabatic Hypothesis, with Allowance for the Participation of Excited Particles in the Process

Process $A^+ \rightarrow A^-$

Let us first carry out the analysis of the curves of $\sigma_{1-1}(v)$ for two-electron charge transfer to ions in inert gases. It is natural to begin this analysis with the simplest case, in which the particles involved can be only in their ground states. This simplest case occurs only for the one combination $H^+ - He$.

The resonance defect for process (III) is calculated by Eq. (3); for the combination $H^+ - He$ it is equal to 64.4 ev. After determining v_{max} from the curve of $\sigma_{1-1}(v)$ in Fig. 2 we can use the condition (2) to calculate the quantity a. For the combination $H^+ - He$ its value is 1.6 A.

The analysis of the curves of $\sigma_{1-1}(v)$ for the process $H^+ \rightarrow H^-$ in Ne, Ar, Kr, and Xe is complicated by the fact that in these cases two-electron charge transfer to the proton can be accompanied by the formation of an excited slow doubly charged ion. In other words, two-electron charge transfer to a proton can occur not only by the process (III) but also by the process

$$A^* + B \rightarrow A^- + B^{++*}, \qquad (V)$$

whose resonance defect must be calculated from the formula

$$\Delta E_1 = (S_A + V_A^I) - (V_B^I + V_B^{II} + E_{B^{++}}), \qquad (12)$$

where $E_{B^{++}}$ is the excitation energy of the ion B^{++}. A comparison of (3) and (12) shows that

$$|\Delta E_0| < |\Delta E_1|. \qquad (13)$$

The inequality (13) shows that if the constant a has the same value for processes (III) and (V) the maximum of the curve of $\sigma_{1-1}(v)$ for process (III) must lie at a smaller velocity than that for process (V). With this in mind we can explain the shape of the curves in Fig. 3 in the following way: the experimentally observed curve of $\sigma_{1-1}(v)$ is the resultant of a number of curves, which correspond to two-electron charge transfer to protons with the formation of doubly charged ions in the ground state and in various excited states. If we accept this interpretation of the curves of Fig. 3, then the narrow maximum at the smaller velocity corresponds to

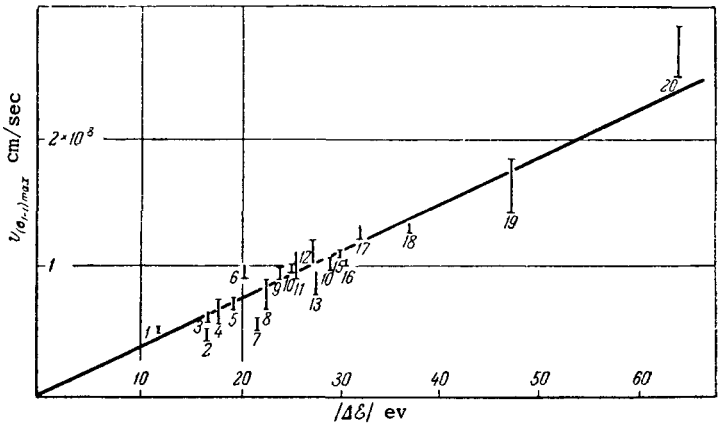

FIG. 10. 1 – $F^+ - Xe$; 2 – $F^+ - Kr$; 3 – $Cl^+ - Xe$; 4 – $O^+ - Xe$; 5 – $H^+ - Xe$; 6 – $C^+ - Xe$; 7 – $F^+ - Ar$; 8 – $O^+ - Kr$; 9 – $H^+ - Kr$; 10 – $B^+ - Xe$; 11 – $C^+ - Kr$; 12 – $Li^+ - Xe$; 13 – $O^+ - Ar$; 14 – $H^+ - Ar$; 15 – $B^+ - Kr$; 16 – $C^+ - Ar$; 17 – $Li^+ - Kr$; 18 – $Li^+ - Ar$; 19 – $H^+ - Ne$; 20 – $H^+ - He$.

process (III) and the broad maximum arises from the superposition of a number of curves of $\sigma_{1-1}(v)$ for processes (V) that give B^{++} ions with various energies of excitation.

Our attention is caught by the decrease of the relative height of the second maximum for the combinations $H^+ - Xe$, $H^+ - Kr$, $H^+ - Ar$, and $H^+ - Ne$ with decrease of the atomic number of the gas. In Ne this maximum does not appear at all, and the effect of the processes (V) leads only to the asymmetry of the curve of $\sigma_{1-1}(v)$ which was mentioned earlier.

Starting from the assumption that the maxima at the lower velocities for the combinations $H^+ - Ar$, $H^+ - Kr$, and $H^+ - Xe$, and also the maximum for the combination $H^+ - Ne$, correspond to processes of two-electron charge transfer in which all of the particles are in their ground states, we can use the adiabatic criterion (2) to calculate values of a for all of these combinations. The calculation shows that these values are all approximately the same for the process $H^+ \rightarrow H^-$ in the five inert gases; they vary around an average value of 1.5 A.

This lack of dependence of the constant a on the nature of the pair of colliding particles holds also for other ions, as can be seen if we make a plot of values of v_{max} against $|\Delta E|$. It follows from the criterion (2) that if a is the same for the various ion-atom combinations, then $v_{max} \sim |\Delta E|$. How well the linear relation between the quantities v_{max} and $|\Delta E|$ holds can be seen from Fig. 10, where the relation has been plotted for the 20 ion-atom combinations for which a maximum of the curve of $\sigma_{1-1}(v)$ was observed.* The vertical bars indicate the errors in the determination of v_{max}. As can be seen from Fig. 10, the points for these combinations straddle a straight line which corresponds to a = 1.5 A. The same result, i. e., approximate constancy of the quantity a for various ion-atom combinations, was obtained in reference 14 for one-electron charge transfer, the only difference being that in that case the value found was a = 8 A.

On the assumption that for two-electron charge-transfer processes involving excited particles the constant a has the same value as for processes involving unexcited particles, we can use the position of the maximum at higher velocity on the curves of $\sigma_{1-1}(v)$ for the combinations $H^+ - Xe$, $H^+ - Kr$, and $H^+ - Ar$ to determine the excitation energy of the doubly charged ion, In fact, it follows from Eqs. (3) and (12) that

$$|\Delta E_1| - |\Delta E_0| = E_{B^{++}}. \qquad (14)$$

Assuming that for process (V) a = 1.5 A, we can use the adiabatic criterion (2) to calculate the quantity $|\Delta E_1|$, and then calculate the quantity $E_{B^{++}}$. It was found that for these combinations the values of $E_{B^{++}}$ agree within the errors of the measurements with the third ionization potentials of the atoms Ar, Kr, and Xe (see Table II).

Thus, on the assumption made, we must suppose that for these ion-atom combinations the second maximum of the curves of $\sigma_{1-1}(v)$ is due to the process

$$H^+ + B \rightarrow H^- + B^{+++} + e. \qquad (VI)$$

According to the terminology proposed in reference 45, we can call process (VI) a process of ionization with capture, in which two of the three electrons removed from particle B are captured by the proton and the third electron goes off into the continuous spectrum.

It can be seen from Fig. 3 that for the combinations $H^+ - Xe$ and $H^+ - Kr$ the height of the maximum of $\sigma_{1-1}(v)$ at the larger velocity is greater than that of the maximum at the smaller velocity. At first sight this fact does not seem readily understandable, since it is hard to believe that process (VI), which has a much larger resonance defect than process (III), can have a larger probability. It must be remembered, however, that the shape of the curve of $\sigma_{1-1}(v)$ in the region between the two maxima is determined not only by processes (III) and (VI) but evidently also by a number of processes of type (V) with various energies of excitation of the B^{++} ions. Therefore the height of the second maximum, being determined by the sum of the

*In the construction of the graph of the relation $v_{max} = f(|\Delta E|)$ the points for the processes $F^+ \rightarrow F^-$ and $B^+ \rightarrow B^-$ were plotted on the assumption that the maximum at the largest velocity corresponds to the two-electron charge-transfer process in which all the particles are in their ground states. The basis for this choice will be clear from the further discussion.

TABLE II

Ion-Atom combination	$\lvert\Delta E_1\rvert - \lvert\Delta E_0\rvert$ in ev	V_B^{III} in ev
$H^+ - Xe$	30.0	31.3
$H^+ - Kr$	33.5	35.7
$H^+ - Ar$	39.0	40.9

cross sections of the processes of type (V) and that of type (VI), can be of the same order of magnitude as the height of the first maximum, or even larger.

A more detailed idea of the various processes of two-electron charge transfer to protons in heavy inert gases that determine the shapes of the curves of $\sigma_{1-1}(v)$ could be obtained by studying the energy losses that occur in the endothermal process of conversion of positive ions into negative ions.*

We next elucidate the causes of the appearance of two maxima on the curves of $\sigma_{1-1}(v)$ for the combinations $F^+ - H_2$, $F^+ - Ar$, $F^+ - Kr$, $F^+ - Xe$, $O^+ - Xe$, and for the appearance of three maxima for the combinations $B^+ - H_2$, $B^+ - Kr$, and $B^+ - Xe$.

First of all it must be emphasized that for the processes $F^+ \rightarrow F^-$ and $B^+ \rightarrow B^-$ the appearance of several maxima on the curves of $\sigma_{1-1}(v)$ cannot be explained by the production of excited doubly charged ions, as it can in the case of $H^+ \rightarrow H^-$ processes in Ar, Kr, and Xe. This possibility is excluded by the fact that the curves of $\sigma_{1-1}(v)$ for the combinations $F^+ - H_2$ and $B^+ - H_2$ have two and three maxima, respectively, just like the corresponding curves for the processes $F^+ \rightarrow F^-$ and $B^+ \rightarrow B^-$ in the noble gases. For two-electron charge transfer in hydrogen, however, the production of excited slow ions is impossible, so that the complex structure of the curves of $\sigma_{1-1}(v)$ has a different cause. This cause is the presence of an admixture of metastable excited ions in the primary beam. The process

$$A^{++} + B \rightarrow A^- + B^{++} \qquad \text{(VII)}$$

(two-electron charge transfer to an excited ion) has the resonance defect

$$\Delta E_2 = (S_A + V_A^I + E_{A^+}) - (V_B^I + V_B^{II}), \qquad (15)$$

where E_{A^+} is the energy of excitation of the ion.

It follows from a comparison of the formulas (3) and (15) that for all $E_{A^+} < 2\lvert\Delta E_0\rvert$ we have the inequality

$$\lvert\Delta E_0\rvert > \lvert\Delta E_2\rvert. \qquad (16)$$

The inequality (16) shows that if the constant a has the same value for processes (III) and (VII) the maximum of the curve of $\sigma_{1-1}(v)$ for process (III) must lie at a higher energy than the maximum for the processes (VII). For this reason, in the construction of the plots of the relation $v_{max} = f(\lvert\Delta E\rvert)$ (Fig. 10) the points for the processes $F^+ \rightarrow F^-$ in Ar, Kr, and Xe, $B^+ \rightarrow B^-$ in Kr and Xe, and $O^+ \rightarrow O^-$ in Xe were plotted on the assumption that the maximum at the larger velocity corresponds to the process of two-electron charge transfer with all the particles in their ground states.

On the basis of Eqs. (3) and (15) we have the following equation:

$$E_{A^+} = \lvert\Delta E_0\rvert - \lvert\Delta E_2\rvert. \qquad (17)$$

By using the adiabatic criterion (2), we can calculate from the velocities at which the additional maxima occur the values of $\lvert\Delta E_2\rvert$, and then can find from Eq. (17) the excitation energies of the ions.

Table III shows a comparison of the excitation energies of the ions found by calculation from the formula (17) with the energies of the corresponding terms found from spectroscopic data.* As can be seen from the table, in all cases except that of the combination $F^+ - H_2$ the calculated values for the excitation energies of the ions agree within the errors of the measurements with the energies of the terms from spectroscopic data. The curve for the combination $F^+ - Xe$ has a maximum associated with the state $2s^2 2p^4\ ^1D$. On the curves for $F^+ - Kr$ and $F^+ - Ar$ the maximum associated with this state is not separated from the main maximum, but there is a maximum from the state $2s^2 2p^4\ ^1S$. Finally, for the combination $F^+ - Ne$ there is a maximum from the state $2s2p^5\ ^3P_0$. All of these states are metastable.

The curves for $B^+ - Xe$, $B^+ - Kr$, and $B^+ - H_2$ show two additional maxima, associated with the states $2s2p\ ^3P_0$ and $2p^2\ ^3P$. According to the selection rules, only the first of these states is metastable. The presence of the maximum associated with the state $2p^2\ ^3P$ of the B^+ ion makes it possible to estimate the order of magnitude of the lifetime T of this state.

It is easy to show that

$$T = \frac{t}{\ln \frac{K_0}{K}}, \qquad (18)$$

where t is the time of flight of the ions from the source to the collision chamber and K_0 and K are the respective concentrations of excited ions in the beam emerging from the source and in the beam entering the collision chamber. Certain data (see below) indicate that a concentration $K \approx 5$ percent is enough for the appearance of a maximum from the excited ions on the curve of $\sigma_{1-1}(v)$. Setting $K_0 \approx 100$ per cent, which is, of course, obviously too high, we can get a very crude lower limit on T. For the state

*It is easy to show that under the conditions $\theta = 0$, $\Delta E \ll T_0$, and $m_1/m_2 \ll 1$ the relation $\Delta T = \lvert\Delta E\rvert$ is valid, where θ and ΔT are the scattering angle and the energy loss in two-electron charge transfer, m_1 and m_2 are the masses of the ion and the gas atom, and T_0 is the kinetic energy of the primary ion. By studying the spectrum of the energy losses in conversions $A^+ \rightarrow A^-$ and using this relation one can calculate the excitation energies of the doubly charged ions produced in the two-electron charge transfers.

*The excitation energies of the ions are taken from reference 46.

TABLE III

Ion-molecule combination	Calculated excitation energy of ion in ev	Designation of term of excited ion	Energy of term from spectroscopic data in ev	Metastable terms of excited ion
F^+-Xe	3.6±0,9	$2s^22p^4\ ^1D$	2.6	$2s^22p^4\ ^1D$
F^+-Kr	6.5±1,6	$2s^22p^4\ ^1S$	5.6	$2s^22p^4\ ^1S$
F^+-Ar	6.3±1,9	$2s^22p^4\ ^1S$	5.6	$2s2p^5\ ^3P_0$
F^+-Ne	20.4±2,0	$2s2p^5\ ^3P^0$	20.5	
F^+-H_2	10.0±2,0			
B^+-Xe	5.0±0,9	$2s2p\ ^3P^0$	4.6	$2s2p\ ^3P^0$
B^+-Xe	11.3±1,0	$2p^2\ ^3P$	12.1	
B^+-Kr	5.6±1,6	$2s2p\ ^3P^0$	4.6	
B^+-Kr	11.7±1,6	$2p^2\ ^3P$	12.1	
B^+-H_2	4.4±0,3	$2s2p\ ^3P^0$	4.6	
B^+-H_2	11.0±2,0	$2p^2\ ^3P$	12.1	
O^+-Xe	24.2±0,5	$2s2p^4\ ^2S$	24.4	$2s^22p^3\ ^2D_{5/2,\ 3/2}$ $2s^22p^3\ ^2P^0_{3/2,\ 1/2}$ $1s2s\ ^3S$
Li^+-Kr	59.9±2,0	$1s2s\ ^3S$	59.0	$1s2s\ ^1S$
		$1s2s\ ^1S$	60.7	
Li^+-Ar	61.3±2,0	$1s2s\ ^3S$	59.0	
		$1s2s\ ^1S$	60.7	

$2p^2\ ^3P$ of the B^+ ion this lower limit is 5×10^{-7} sec.

For the combination O^+-Xe there is a maximum associated with the nonmetastable excited state $2p^4\ ^2S$. According to the crude method of estimation just described, a lower limit on the lifetime of this state is of the order of 10^{-6} sec. Since the curve of $\sigma_{1-1}(v)$ for the combination O^+-Xe shows a maximum from this nonmetastable state of the O^+ ion, it is obvious that at O^+ ions in the primary beam must be in the metastable states $2s^22p^3\ ^2D_{5/2,\ 3/2}$ and $2s^22p^3\ ^2P^0_{3/2,\ 1/2}$. The maxima associated with these states, however, are displaced from the main maximum by 3.3 and 5 ev, respectively, and therefore are not separated from it. The presence of ions in these excited states in the primary beam leads only to a broadening of the main maximum, which is indeed observed on the curves of $\sigma_{1-1}(v)$ for the process $O^+ \rightarrow O^-$.

The analysis of the $\sigma_{1-1}(v)$ curves that has been given provides a basis for the supposition that the Massey adiabatic criterion can be applied to processes $A^+ \rightarrow A^-$, with the further hypothesis that the value of the constant a for such a process is the same, independently of whether or not excited particles are involved. These assumptions receive indirect confirmation in the experiments that have been described. It is, however, possible to make a direct experiment to get evidence on the correctness of the assumptions made in the interpretation of the shapes of the curves of $\sigma_{1-1}(v)$. The experiment consists of a comparison of the curves of $\sigma_{1-1}(v)$ for a given pair of colliding particles but for ions obtained from different ion sources—a thermionic source and a high-frequency source. The idea of this experiment is based on the fact that an ion beam obtained from a thermionic source surely does not contain excited ions, whereas a beam obtained from a high-frequency source can contain excited ions. Owing to this a curve of $\sigma_{1-1}(v)$ obtained with an ion beam from a thermionic source should show no additional maxima associated with the presence of ions in excited states in the primary beam, but these maxima can appear on the corresponding curve obtained with a beam from a high-frequency source.

In this respect the most unambiguous results should be given by the curves of $\sigma_{1-1}(v)$ for the process $Li^+ \rightarrow Li^-$, since the Li^+ ion has only two metastable states, $2s^3S$ and $2s^1S$, with nearly equal excitation energies 59 and 60.7 ev, which for some combinations give additional maxima located not far from the main maximum. The results of the comparison of the curves of $\sigma_{1-1}(v)$ for the process $Li^+ \rightarrow Li^-$ in Kr, Ar, and H_2 are shown in Fig. 11. The curve obtained with the thermal source has only one maximum, which is due to the process $Li^+ \rightarrow Li^-$ for the Li^+ ion in its ground state. On the curve obtained with the high-frequency source (drawn with dashed line) there is an additional maximum associated with the presence in the beam of Li^+ ions in the excited states $2s^3S$ and $2s^1S$. The arrows on the diagrams show the positions of the maxima* for the processes $Li^+\ (^3S) \rightarrow Li^-$ and $Li^+\ (^1S) \rightarrow Li^-$, as calculated on the basis of the Massey adiabatic criterion, on the assumption that for these processes the constant a has the same value, of the order of 1.5 A, as for the process $Li^+ \rightarrow Li^-$ that fixes the position of the main maximum. As can be seen from Fig. 11, within the errors of measurement the additional maxima for Kr and Ar are at the places predicted for them by the Massey adiabatic criterion.† We conclude from this that the assumption

*Because of the small difference of the energies of the terms $2s^3S$ and $2s^1S$ the additional maxima associated with these states are not separated.

†It was not possible to establish the position of the additional maximum on the curve of $\sigma_{1-1}(v)$ for H_2, because of the low intensity of the Li^+ beam at low energies, but it can be seen from the curve that this maximum exists.

Li^+ and Na^+ ions,* so that the fraction of excited ions in the K^+ beam is larger than in the Li^+ and Na^+ beams. The detection of the side maximum on the curves of $\sigma_{1-1}(v)$ for the process $K^+ \rightarrow K^-$ is facilitated by the circumstance that the side maximum lies very far from the main maximum [for the combination $K^+ \rightarrow K^-$ (sic) these maxima are at energies 40 and 306 ev, respectively]. Owing to this, in the neighborhood of the side maximum $\alpha \gg 1$, therefore it follows from Eq. (20) that

$$\frac{\sigma'_{1-1}-\sigma_{1-1}}{\sigma_{1-1}} = K\alpha,$$

that is, the side maximum can be detected even for small K, provided α is large enough.

The foregoing analysis shows that, for all the combinations studied for which the curves of $\sigma_{1-1}(v)$ have complex structures, these structures can be explained by means of the Massey adiabatic criterion, on the basis of the fact that in addition to two-electron charge-transfer processes in which all the particles are in their ground states there occur also two-electron charge-transfer processes involving excited particles.

Maxima on the curves of $\sigma_{1-1}(v)$ are also observed in some cases of two-electron charge transfer in molecular gases (the processes $H^+ \rightarrow H^-$, $Li^+ \rightarrow Li^-$, $B^+ \rightarrow B^-$, $F^+ \rightarrow F^-$, and $O^+ \rightarrow O^-$ in H_2 and $H^+ \rightarrow H^-$ and $Cl^+ \rightarrow Cl^-$ in N_2). In the discussion of two-electron charge transfer in molecular gases it must be remembered that this process can occur in two different ways, which can be represented schematically by the formulas

$$A^+ + B_2 \rightarrow A^- + B_2^{++}, \qquad \text{(VIII)}$$

$$A^+ + B_2 \rightarrow A^- + B^+ + B^+. \qquad \text{(IX)}$$

The resonance defect of process (VIII), in which a slow doubly charged molecular ion is produced,† can be calculated from Eq. (3). As for process (IX), its resonance defect must be calculated from the formula

$$\Delta E = V_A^I + S_A - (E_{diss} + 2V_B^I + E_p), \qquad (21)$$

where E_{diss} is the dissociation energy of the molecule B_2, and E_p is the potential energy of the two B^+ ions that are formed. It is easy to see that two-electron charge transfer in hydrogen can occur only by process (IX). In this case the resonance defect can be calculated unambiguously, since the value of E_p for two protons produced from an unexcited H_2 molecule is known.[48] The situation is different for other molecular gases, for which the value of E_p is unknown, and therefore the resonance defect can be calculated only for the process that goes according to the scheme (VIII), and even here only provided the first and second ionization potentials of the molecule B_2 are known.

Table IV shows values of the constant a for two-electron charge transfer in molecular gases, as calculated on the basis of the adiabatic criterion (2). For the combinations $H^+ - N_2$ and $Cl^+ - N_2$ it was assumed that the two-electron charge-transfer process goes according to the scheme (VIII), and the calculations of the resonance defects were made by using the potential for appearance of the ion N_2^{++} as found in reference 49.

TABLE IV

Ion-molecule combination	a in A
$H^+ - H_2$	2.3
$O^+ - H_2$	0.9
$F^+ - H_2$	0.9
$B^+ - H_2$	1.0
$Li^+ - H_2$	0.9
$H^+ - N_2$	2.0
$Cl^+ - N_2$	0.5

The calculations of a for the combinations $B^+ - H_2$ and $F^+ - H_2$ were made on the assumption that the process of double charge transfer to the unexcited ion corresponds to the maximum located at the largest velocity.

As can be seen from Table IV, the values of a for two-electron charge transfer in molecular gases vary over a wide range and differ considerably from the average value of 1.5 A that is characteristic for atomic gases. An analysis of the curves of $\sigma_{1-1}(v)$ for the combinations $B^+ - H_2$ and $F^+ - H_2$ shows that in these cases the constant a is not the same for two-electron charge transfers to the unexcited and excited ions. Thus the dependence of the quantity a on the nature of the colliding particles is different for atomic and molecular gases. For atomic gases this constant depends only weakly on the nature of the colliding particles and on the state of excitation of the ion, but these regularities are not valid for molecular gases. A similar situation has been found by Hasted and his collaborators in the case of one-electron charge transfer to singly-charged positive ions.

Process $A^0 \rightarrow A^-$

Just as for the process $A^+ \rightarrow A^-$, we first make an analysis of the curves of $\sigma_{0-1}(v)$ for the process $A^0 \rightarrow A^-$ in inert gases. This analysis can be made most simply in the case $H^0 \rightarrow H^-$, since in this case it is quite well known that the beam of hydrogen atoms does not contain metastable atoms. The point is that although the hydrogen atom does have the metastable state $2^2S_{1/2}$ with lifetime of the order of 0.1 sec, before entering the collision chamber the neutral beam had passed through an electric field (the capacitor 11 in Fig. 1, for clearing the beam of charged particles). The action of this field decreased the lifetime of the excited state to 2×10^{-8} sec, and owing to this the

*The assertion that the excitation cross sections of alkali-metal ions increase with increasing atomic number is confirmed by the data of reference 47, in which it was shown that the intensities of lines in the spark spectrum of alkali metals which appear when beams of these ions pass through mercury vapor increase with increasing atomic number of the ion.

†Naturally, the process of type (VIII) can occur only in cases in which the ion B_2^{++} is stable.

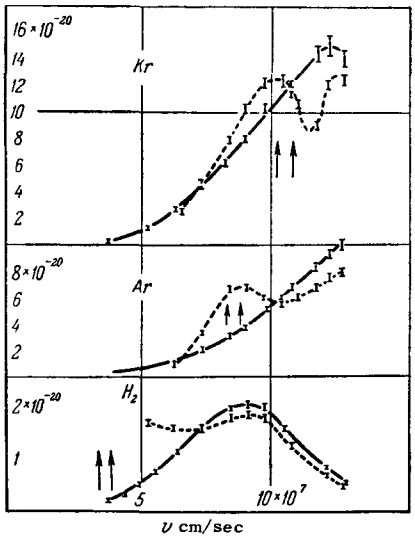

FIG. 11. The process $Li^+ \rightarrow Li^-$. —— thermal source, - - - high-frequency source.

that the constant a is the same for two-electron charge-transfer processes involving unexcited and excited ions is correct. A fact worthy of attention is that, because of the large excitation energy of the Li^+ ion, the resonance defect of the process $Li^+ \rightarrow Li^-$ has a positive value, and this means that the constant a has the same value for endothermal and exothermal processes of two-electron charge transfer. The results of the study of the process $Li^+ \rightarrow Li^-$ demonstrate directly the possibility of applying the Massey adiabatic criterion to processes of two-electron charge transfer in the case of these ions, and also confirms the correctness of the explanation of the nature of the additional maxima on the curves of $\sigma_{1-1}(v)$ for the processes $F^+ \rightarrow F^-$, $B^+ \rightarrow B^-$, and $O^+ \rightarrow O^-$.

A comparison of the curves of $\sigma_{1-1}(v)$ for beams with and without an admixture of ions in excited states gives a possibility of estimating the concentration of excited ions in the primary beam. In fact, if the primary beam contains excited ions with only one excitation energy the cross section σ'_{1-1} for such a beam will be given by the formula

$$\sigma'_{1-1} = K\sigma^*_{1-1} + (1-K)\,\sigma_{1-1}, \qquad (19)$$

where K is the concentration of excited ions and σ^*_{1-1} and σ_{1-1} are the cross sections for two-electron charge transfer to excited and unexcited ions. If we introduce the notation $\alpha = \sigma^*_{1-1}/\sigma_{1-1}$, Eq. (19) can be rewritten in the form

$$\frac{\sigma'_{1-1}}{\sigma_{1-1}} = 1 + K(\alpha - 1). \qquad (20)$$

It follows from Eq. (20) that when $\alpha \ll 1$ we have $K = 1 - (\sigma'_{1-1}/\sigma_{1-1})$. The estimate of K can best be made for combinations for which the velocities at the main and additional maxima are very different. For the process $Li^+ \rightarrow Li^-$ the largest difference between these velocities occurs for the combination $Li^+ - H_2$. An estimate of K from the curves of $\sigma_{1-1}(v)$ for this combination, at velocities $v > v'_{max}$ (v'_{max} is the velocity at the main maximum) gives a value of about 0.2.

As Eq. (20) shows, the shape of the curve of $\sigma_{1-1}(v)$ depends essentially on the value of K. It has been established experimentally that a change of the conditions of operation of the high-frequency source leads to a change of the shape of the curve of $\sigma_{1-1}(v)$; namely, while the positions of the main and additional maxima remain unchanged, the values of the cross section at these maxima are changed. It is obvious that this result is due to a change of the fraction of excited Li^+ ions in the primary beam when the conditions of operation of the high-frequency source are changed.

A difference of the shapes of the curves of $\sigma_{1-1}(v)$ obtained with beams from a thermionic source and a high-frequency source is also observed for the process $Na^+ \rightarrow Na^-$ (Fig. 6). The main maximum for this process is located at an energy of 130 kev ($Na^+ - Xe$) or more, i.e., it is outside the range of energies that has been investigated. The simplest combination is $Na^+ - H_2$, since in this case it is impossible for excited atoms of the target gas to be produced. The maximum on the curve in the case of the high-frequency source is due to the presence of primary Na^+ ions in the metastable excited states $3s_5\,{}^3P_2$ and $3s_3\,{}^3P_0$ (sic), which have nearly equal excitation energies. The shape of the curves of $\sigma_{1-1}(v)$ for the process $Na^+ \rightarrow Na^-$ in Ar, Kr, and Xe that are obtained with the beam from the high-frequency source can be explained by occurence of processes of two-electron charge transfer to excited Na^+ ions in the states $3s_5\,{}^3P_2$ and $3d^3F_4$ with simultaneous production of excited doubly-charged ions of the target gas. As estimated from the curves of $\sigma_{1-1}(v)$ for the combination $Na^+ - H_2$, the fraction of Na^+ ions in the states $3s_5\,{}^3P_2$ and $3s_3\,{}^3P_0$ in the primary beam is about 0.25.

In the study of the process $K^+ \rightarrow K^-$ it was found that the curves of $\sigma_{1-1}(v)$ for the gases H_2, Kr, and Xe, obtained with beams from thermionic and high-frequency sources, had maxima associated with the presence of metastable excited K^+ ions in the primary beam. It was established by special experiments that the fraction of excited ions in the beam obtained from the thermionic source was not due to excitation of K^+ ions in collisions with residual gas molecules. The possibility is not excluded that the appearance of excited K^+ ions in the beam from the thermionic source is caused by scattering of some of the ions of the beam at the edges of the diaphragms and covers of the mass-monochromator chamber, accompanied by excitation of the scattered ions. The absence of this effect for the ions Li^+ and Na^+ is due to the fact that the excitation energies of the metastable states of the ions Li^+, Na^+, and K^+ are respectively 60, 33, 20, 3 ev (sic), i. e., much smaller for K^+ than for Li^+ and Na^+, and therefore it is to be expected that the cross section for excitation of the K^+ ion is larger than those for excitation of

neutral beam entering the collision chamber did not contain any excited atoms.

In view of this it can be asserted that the process of electron capture by a hydrogen atom can occur either by a process in which all particles are in their ground states

$$A^+ + B \rightarrow A^- + B^+ \quad (X)$$

with the resonance defect

$$\Delta E_0 = S_A - V_B^I, \quad (22)$$

or else with the production of an excited slow ion

$$A + B \rightarrow A^- + B^{+*} \quad (XI)$$

with the resonance defect

$$\Delta E_1 = S_A - (V_B^I + E_{B^+}), \quad (23)$$

where E_{B^+} is the excitation energy of the B^+ ion.

The question arises as to which of these processes is responsible for the maxima on the curves of $\sigma_{0-1}(v)$ in Fig. 7. If we assume that these maxima are due to process (XI), with excitation of the lowest excited level of the ion B^+, than by using the Massey adiabatic criterion one gets for the combinations $H^0 - He$, $H^0 - Ne$, $H^0 - Ar$, and $H^0 - Kr$ roughly equal values of the constant a, with an average of 1.3 A. Assuming that this value of a remains the same for processes $H^0 \rightarrow H^-$ accompanied by excitation of higher levels of the ion B^+, we can use the Massey criterion to calculate the positions of the maxima for these processes. For the combination $H^0 - Ar$, such a calculation shows that there must be a rather large number of maxima in the energy range 4 — 10 kev, i. e., the curve of $\sigma_{0-1}(v)$ must have a broad maximum in this region. Actually, however (see Fig. 7), the cross section σ_{0-1} falls off rather rapidly from 4 to 10 kev. The situation is similar for the process $H^0 \rightarrow H^-$ in the other inert gases. The assumption that the maximum on the curve of $\sigma_{0-1}(v)$ is due to process (XI) is also contradicted by the shape of the curves for the process $O^0 \rightarrow O^-$. For example, if we assume that for the combination $O^0 - Ar$ the maximum on the curve of $\sigma_{0-1}(v)$ at 55 kev corresponds to process (XI), with excitation of the lowest level of the Ar^+ ion, then the maximum for process (X) must appear at an energy of about 17 kev. Actually, beginning at 10 kev, the cross section σ_{0-1} for the combination $O^0 - Ar$ rises steadily with increasing energy (Fig. 27). This assumption about the nature of the maximum also leads to a contradiction with the actual shape of the curves of $\sigma_{0-1}(v)$ for the process $O^0 \rightarrow O^-$ in Kr and Xe.

Thus we arrive at the conclusion that the maxima on the curves of $\sigma_{0-1}(v)$ for the process $H^0 \rightarrow H^-$ are due to a process of electron capture in which the slow ion remains in the ground state [process (X)]. For this process in inert gases the constant a turns out to be about 3 A. It must be noted that for the process $H^0 \rightarrow H^-$ in molecular gases, unlike the processes of two-electron charge transfer, the constant a is the same as for atomic gases (see discussion of Fig. 12), if we assume that capture of the electron from the molecule is accompanied by dissociation of the molecular ion.

We can point out one further difference between the processes $H^0 \rightarrow H^-$ and $H \rightarrow H^-$ in inert gases. As was mentioned earlier, in the case of the process $H^+ \rightarrow H^-$ processes in which slow excited ions are produced have a rather large effect on the shape of the curve of $\sigma_{1-1}(v)$; this leads to the appearance of a broad additional maximum, and in the cases of Ar, Kr, and Xe the height of this maximum is larger than or comparable with that of the main maximum (Fig. 3). Nothing like this happens in $H^0 \rightarrow H^-$ processes. For example, in the case of the combination $H^0 - Ar$ the production of an excited Ar^+ ion as a result of the process $H^0 \rightarrow H^-$ should give a supplementary maximum in the range 15 — 35 kev. Turning to the curve of $\sigma_{0-1}(v)$ for this combination (Fig. 7) we see that in this energy range there is only some slowing down of the decrease of the cross section σ_{0-1} with increase of the energy of the atom. From this comparison we can conclude that the relative probability of processes $H^0 \rightarrow H^-$ with production of slow excited ions is smaller than that for $H^+ \rightarrow H^-$ processes in the same gases.

Passing now to the analysis of the curves of $\sigma_{0-1}(v)$ for processes of electron capture by He, B, C, O, and F atoms, we must keep in mind the fact that the atomic beam used for the measurement of the cross section σ_{0-1} was obtained by neutralization of a beam of the corresponding singly-charged positive ions in a mercury-vapor target. Since the capture of an electron by a positive atom that collides with a mercury atom can lead to either the ground level or an excited level, the neutral beam formed by passage through the mercury-vapor target can contain metastable excited atoms. The concentration of metastable atoms in the neutral beam depends on the probabilities of the processes that lead to the production and disappearance of unexcited and excited atoms. Furthermore, for target thicknesses that are neither so small that there are single collisions of ions with mercury atoms nor so large that the beam emerging from the target is of equilibrium composition with respect to the excited states, the concentration of excited atoms will depend on the thickness of the target. Since, as is seen in Eq. (19), the measured value of the cross section depends on the concentration K of excited particles in the primary beam, in the range of target thicknesses that has been indicated the measured cross section must depend on K (sic). The absence of such a dependence allows us to conclude that the concentration of excited atoms in the neutral beam is small.

A study of the dependences of the cross sections σ_{0-1} and σ_{01} on the thickness of the mercury target in the cases of He, B, C, O, and F atoms has shown that for all these atoms except He the cross sections

σ_{0-1} and σ_{01} did not depend on the target thickness. Thus only the beam of He atoms contained an appreciable number of atoms in excited states.

The above analysis makes it appear very probable that the maxima on the curves of $\sigma_{0-1}(v)$ for the processes $O^0 \rightarrow O^-$ in Ar, Kr, and Xe, $C^0 \rightarrow C^-$ in Kr and Xe, and $F^0 \rightarrow F^-$ in Kr and Xe, and also the plateaus on the curves of $\sigma_{0-1}(v)$ for the process $B_0 \rightarrow B^-$ in Kr and Xe (see Fig. 9), must be ascribed to process (X), with all the particles in their ground states.

On this assumption we can calculate the constant a for the combinations just enumerated. The result of this calculation is that the values of a do not differ much from the average value 3 A that was obtained for the process $H^0 \rightarrow H^-$ in the inert gases. The degree of deviation of the values of a for various atom-atom combinations from this average value can be seen from Fig. 12, where values of v_{max} are plotted against $|\Delta E|$, and the slope of the straight line corresponds to the value 3 A for the constant a.

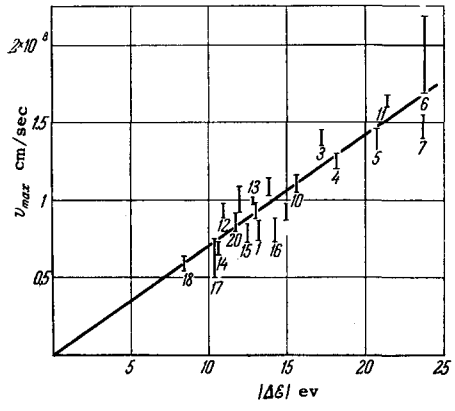

FIG. 12. Processes: 1 – $H^0 \rightarrow H^-$ in Kr; 2 – $H^0 \rightarrow H^-$ in Ar; 3 – $H^0 \rightarrow H^-$ in H_2; 4 – $H^0 \rightarrow H^-$ in O_2; 5 – $H^0 \rightarrow H^-$ in Ne; 6 – $H^0 \rightarrow H^-$ in He; 7 – $H^0 \rightarrow H^-$ in N_2; 8 – $He^0 \rightarrow He^-$ in Xe; 9 – $He^0 \rightarrow He^-$ in Kr; 10 – $He^0 \rightarrow He^-$ in Ar; 11 – $He^0 \rightarrow He^-$ in Ne; 12 – $C^0 \rightarrow C^-$ in Xe; 13 – $C^0 \rightarrow C^-$ in Kr; 14 – $O^0 \rightarrow O^-$ in Kr; 15 – $O^0 \rightarrow O^-$ in Kr; 16 – $O^0 \rightarrow O^-$ in Ar; 17 – $F^0 \rightarrow F^-$ in Kr; 18 – $F^0 \rightarrow F^-$ in Xe; 19 – $B^0 \rightarrow B^-$ in Kr; 20 – $B^0 \rightarrow B^-$ in Xe.

It must be noted that the constant a for the process $A^0 \rightarrow A^-$ is quite different from the value for the process $A^+ \rightarrow A^-$; this is shown particularly clearly in Fig. 13, where of $v_{max} = f(|\Delta E|)$ is plotted for the two processes in the same diagram. In turn, the values of a for the processes $A^0 \rightarrow A^-$ and $A^+ \rightarrow A^-$ are much smaller than that for the process $A^+ \rightarrow A^0$, which, as has already been mentioned, is 8 A, according to the data of Hasted and his co-workers. Thus the results of studies of the processes $A^+ \rightarrow A^0$, $A^+ \rightarrow A^-$, and $A^0 \rightarrow A^-$ enable us to formulate the conclusion that the constant a that appears in the Massey adiabatic criterion depends essentially on the type of process, and depends only weakly on the nature of the pair of colliding particles.

In interpreting the shapes of the curves of $\sigma_{0-1}(v)$ for the process $He^0 \rightarrow He^-$ we must take into account the presence in the beam of He atoms of metastable atoms in the states $2s\ ^1S$ and $2s\ ^3S$. The presence of such atoms has the consequence that along with the process of electron capture by atoms in the ground state there will occur the process

$$A^{0*} + B \rightarrow A^- + B^+, \qquad \text{(XII)}$$

i. e., the process of capture of an electron by an excited atom. The resonance defect of this process is found from the formula

$$\Delta E_2 = (S_A + E_A) - V_B^I, \qquad (24)$$

where E_A is the excitation energy of atom A.

It follows from a comparison of Eqs. (24) and (22) that for all $E_A < 2|\Delta E_0|$ we have the inequality

$$|\Delta E_0| > |\Delta E_2|. \qquad (25)$$

It follows from the inequality (25) that, with the same value of the constant a for processes (XII) and (X), the maxima on the curves of σ_{0-1} caused by processes of type (XII) are at lower velocities than the maxima for process (X).

In considering the curves of $\sigma_{0-1}(v)$ for the processes $He^0 \rightarrow He^-$ in Ne, Ar, Kr, and Xe (cf. Fig. 8) we shall start from the assumption that the observed

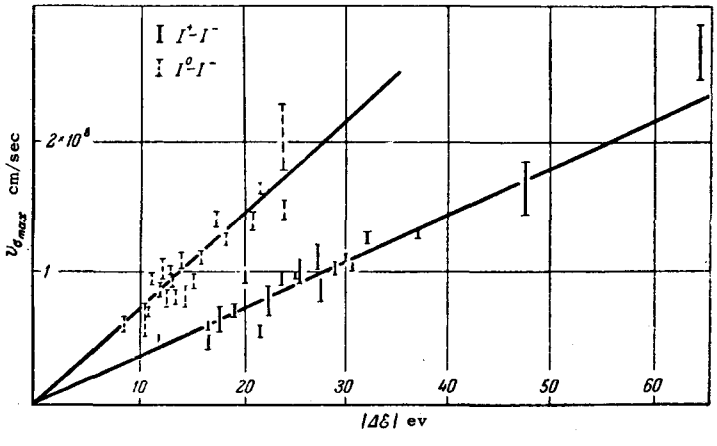

FIG. 13

maxima are due to electron capture by excited He atoms in the metastable states $2s\ ^1S$ and $2s\ ^3S$.* On the hypothesis stated above, the values of a for these processes are close to 3 A, as can be seen from Fig. 12. Thus the assumption that there are metastable atoms in the beam of He atoms is confirmed both by the experiments described earlier, which established the dependence of the cross section σ_{0-1} on the thickness of the mercury target, and also by the existence of supplementary maxima on the curves of $\sigma_{0-1}(v)$ for the process $He^0 \rightarrow He^-$ in Ne, Ar, Kr, and Xe. For the process $He^0 \rightarrow He^-$ the further increase of $\sigma_{0-1}(v)$ after it passes through its maximum is explained by the presence of maxima in the region of higher velocities, associated with processes (X) and (XI). For the process $B^0 \rightarrow B^-$ in Kr and Xe (cf. Fig. 9) the further increase of $\sigma_{0-1}(v)$ after passing through a plateau is explained by the presence at higher velocities of maxima associated with processes of type (XI).

Let us formulate the main conclusions that follow from the analysis of the curves of $\sigma_{1-1}(v)$ and $\sigma_{0-1}(v)$ on the basis of the Massey adiabatic criterion.

1. The adiabatic criterion of Massey can be used to determine the positions of maxima on the curves of $\sigma_{1-1}(v)$ and $\sigma_{0-1}(v)$.

2. For a large number of pairs of colliding particles the constant a that appears in this criterion has average values of 1.5 A and 3 A for the processes $A^+ \rightarrow A^-$ and $A^0 \rightarrow A^-$; that is, it depends essentially on the type of process, and not on the nature of the pair of colliding particles.

3. The constant a is approximately the same for processes involving particles in their ground states and processes involving excited particles.

4. The shapes of the curves of $\sigma_{1-1}(v)$ and $\sigma_{0-1}(v)$ that have complicated structures can be completely explained by the fact that not only particles in their ground states but also particles in excited states can be involved in the processes $A^+ \rightarrow A^-$ and $A^0 \rightarrow A^-$.

c) Behavior of the Curve of $\sigma(v)$ in the Low-Velocity Region

Process $A^+ \rightarrow A^-$

It has been established in the preceding chapter that for the processes $A^+ \rightarrow A^-$ and $A^0 \rightarrow A^-$ the position of a maximum on the curve of $\sigma(v)$ is determined by the Massey adiabatic criterion. A second, perhaps more important requirement of the adiabatic hypothesis is that in the low-velocity region ($a|\Delta E|/hv \gg 1$) the variation of the cross section with velocity should follow a definite law, which is expressed by Eq. (1) and can be written in the different form:

$$\ln \sigma = \ln \sigma_0 - \frac{ka|\Delta E|}{h}\frac{1}{v}. \qquad (26)$$

Thus if for a given process there is a linear relation between the quantities $\ln\sigma$ and $1/v$ in the low-velocity region, then the adiabatic hypothesis can be applied to the process. From the tangent of the angle of inclination of the graph of this linear dependence one can determine the product of the constants k and a. If the constant a for the same process is independently determined from the position of a maximum, the constant k in Eq. (1) can be calculated.

In considering the question of the behavior of the curve of $\sigma_{1-1}(v)$ in the low-velocity region we must first of all remember that the behavior of the curve in this region can be distorted owing to the presence of excited ions in the primary ion beam. Such a distortion will occur in cases in which the additional maxima associated with two-electron charge transfer to excited ions can fall in the adiabatic region. For this reason, in finding the law of variation of σ_{1-1} as a function of v in the low-velocity region we cannot use the curves of $\sigma_{1-1}(v)$ for the process $K^+ \rightarrow K^-$ (see above), nor the curves of $\sigma_{1-1}(v)$ for $Na^+ \rightarrow Na^-$ and $Li^+ \rightarrow Li^-$ obtained with the beam from the high-frequency source (cf. Figs. 6 and 11).

Distortion of the behavior of the curve of $\sigma_{1-1}(v)$ in the adiabatic region can also occur in cases when the process of two-electron charge transfer can give excited slow ions. Such a distortion is most probable when the additional maxima associated with these processes are located near the main maximum and the range of velocities studied is not far enough from the main maximum.

On the basis of this discussion we can conclude that the best curve for settling the question of the law of variation of the cross section σ_{1-1} in the low-velocity region is the curve of $\sigma_{1-1}(v)$ for the process $Na^+ \rightarrow Na^-$ in H_2, with the beam of Na^+ ions obtained from the thermionic source. This conclusion is based on the fact that, on one hand, distortion of the adiabatic region is excluded because in this case excited particles can play no part in the two-electron charge-transfer process, and, on the other hand, the points on the curve of $\sigma_{1-1}(v)$ for this case correspond to the largest values of the parameter $a|\Delta E|/hv$.

The graph of the relation $\ln\sigma = f(1/v)$ for the process $Na^+ \rightarrow Na^-$ in H_2 is shown in Fig. 14. As can be seen from this graph, a number of the points fit well on a straight line. The points for the smallest velocities, however, beginning at the velocity 4.1×10^7 cm/sec, deviate more and more from this line as the velocity of the ion becomes smaller. This deviation from the linear relation between $\ln\sigma$ and $1/v$ at small velocities is not accidental, since the curves of $\ln\sigma = f(1/v)$ for the process $Na^+ \rightarrow Na^-$ in Ar, Kr, and Xe have altogether the same shape as for the process in H_2.

The situation is similar for the process $Li^+ \rightarrow Li^-$, as can be seen from Fig. 15, which shows a graph of the relation $\ln\sigma_{1-1} = f(1/v)$ for this process in H_2

*Because of the small difference between the energies of the terms $2s\ ^1S$ and $2s\ ^3S$ the maxima caused by the two processes are not separated.

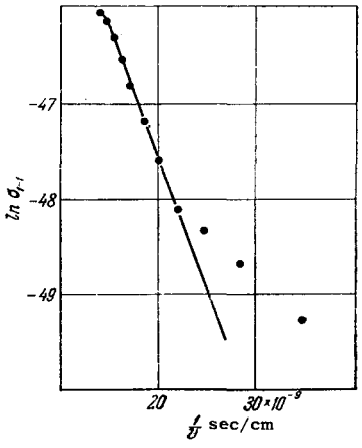

FIG. 14. The process $Na^+ \rightarrow Na^-$ in H_2.

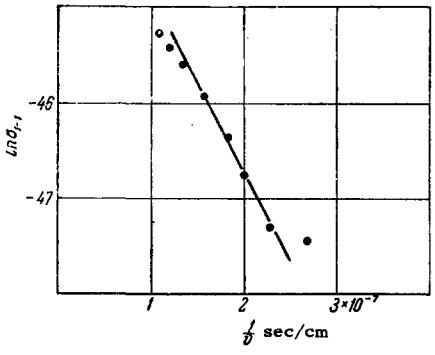

FIG. 15. The process $Li^+ \rightarrow Li^-$ in H_2.

(beam of Li^+ ions from thermionic source). In this case there are deviations from the straight line for two points in the region of the maximum [the point with the smallest value of 1/v corresponds to the maximum of the curve of $\sigma_{1-1}(v)$] and for one point at the smallest velocity (3.7×10^7 cm/sec) of the range investigated. The graphs for the process $Li^+ \rightarrow Li^-$ in Ar, Kr, and Xe show a similar behavior.

Violations of the adiabatic law of decrease of cross section with decrease of velocity in the region of small velocities, where this law should hold most exactly, also occur for the process $A^0 \rightarrow A^-$ (see below) and $A^+ \rightarrow A^0$.[17] Papers devoted to the ionization and excitation of atoms by ionic impacts also describe a sharp reduction of the rate of decrease of the cross sections in the low velocity region.[50, 51] Evidently the violation of the adiabatic law (1) in the low velocity region is due to some cause that is common to all of these processes; we return to its elucidation later, after our consideration of the graphs of $\ln \sigma = f(1/v)$ for the process $A^0 \rightarrow A^-$.

Attention must be called to one other peculiarity of the curves of $\sigma_{1-1}(v)$ in the region $v < v_{max}$. It turns out that the behavior of these curves satisfies Eq. (1) for points quite near to the maximum (cf. Fig. 15), i. e., for velocities for which the condition $a|\Delta E|/hv \gg 1$ is not satisfied.

It is interesting to see how the nature of the pair of colliding particles affects the rate of fall of the cross section in the region where Eq. (1) holds; this rate is

TABLE V

Ion-molecule combination	a in A	ka in A	k
Li^+-H_2	0.9	1.8	2.0
Li^+-Ar		2.2	
Li^+-Kr	1.4	3.1	2.2
Li^+-Xe	1.7	4.0	2.4
Na^+-H_2		2.6	
Na^+-Ar		2.3	
Na^+-Kr		3.1	
Na^+-Xe		3.8	

fixed by the constant k in the formula. Table V shows the values of the product ka for the processes $Na^+ \rightarrow Na^-$ and $Li^+ \rightarrow Li^-$ in H_2, Ar, Kr, and Xe, as calculated from the slope of the linear part of the graph of the relation $\ln \sigma_{1-1} = f(1/v)$. For those ion-molecule combinations for which the maximum of the curve of $\sigma_{1-1}(v)$ is reached, the values of the constants a and k are also given separately.

From the data of Table V we can draw the following conclusions about two-electron charge transfer in inert gases: 1) the product ka has only a weak dependence on the nature of the alkali-metal ion, and 2) ka increases with increasing atomic number of the target gas. Since the constant a depends weakly on the nature of the colliding particles, the quantity k also increases with increase of the atomic number of the target gas. In this respect two-electron charge transfer differs from one-electron charge transfer, for which the constant k has a weak dependence on the nature of the ion-atom combination.[17]

Process $A^0 \rightarrow A^-$

The curves of $\sigma_{0-1}(v)$ that are most useful for finding the law of variation of the cross section σ_{0-1} with the velocity of the atom in the low-velocity region are those for the processes $B^0 \rightarrow B^-$, $C^0 \rightarrow C^-$, $O^0 \rightarrow O^-$, and $F^0 \rightarrow F^-$ in He and Ne. The justification for this assertion is that the beams of B, C, O, and F atoms do not contain appreciable numbers of metastable excited atoms, and consequently the possibility is excluded that the behavior of the curve of $\sigma_{0-1}(v)$ is distorted in the range of velocities in which we are interested by the capture of electrons by excited atoms. On the other hand, the supplementary maxima associated with the production of slow excited ions lie very far from the main maximum, and, as was mentioned previously, this excludes a possibility of distortion of the curve in the low-velocity region. To this we must add that the largest values of the adiabatic parameter $a|\Delta E|/hv$ for processes of electron capture by atoms are those found in the gases He and Ne.

Plots of the relation $\ln \sigma_{0-1} = f(1/v)$ show that for all the indicated processes there is a linear relation between the quantities $\ln \sigma_{0-1}$ and 1/v. How well the points lie on a straight line can be seen from Fig 16, which shows the graph for the combination O – Ne. Only in one case, for the combination B – Ne, was a

departure from the linear dependence observed, for the smallest velocity in the range investigated (Fig. 17).

The values of ka determined from the slopes of the straight lines $\ln\sigma_{0-1} = f(1/v)$ are given in Table VI.

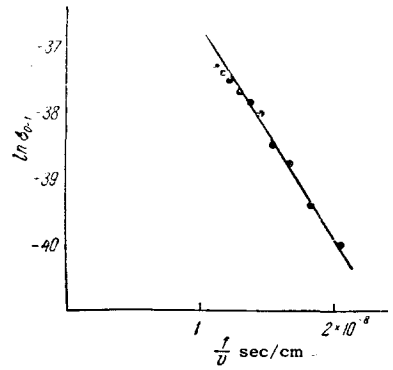

FIG. 16. The process $O^0 \rightarrow O^-$ in Ne.

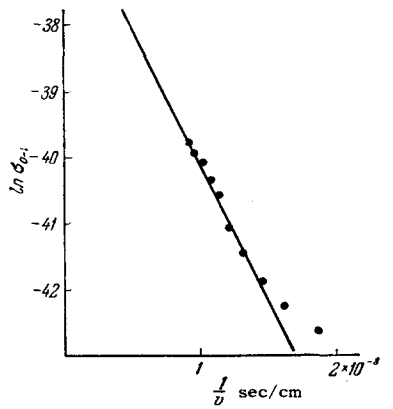

FIG. 17. The process $B^0 \rightarrow B^-$ in Ne.

TABLE VI

Values of ka in A				
Process / Gas	$B^0 \rightarrow B^-$	$C^0 \rightarrow C^-$	$O^0 \rightarrow O^-$	$F^0 \rightarrow F^-$
He	5.1	5.5	4.2	3.8
Ne	6.5	7.0	6.6	4.8

As can be seen from this table, the values of ka increase with increasing atomic number of the target gas. The effect of the nature of the fast atom becomes apparent for the heavy atoms O and F. The quantity ka decreases with increase of the atomic number of the fast ion. The value of ka for the process $A^0 \rightarrow A^-$ is larger than that for $A^+ \rightarrow A^-$, obviously because the constant a is larger for the former process than for the latter. If we recall that the average value of a for processes of the type $A^0 \rightarrow A^-$ is 3 A, we see that the values of k for the processes $A^0 \rightarrow A^-$ and $A^+ \rightarrow A^-$ do not differ very much.

Thus all of the experimental material that is suitable for a judgement on this question shows that the adiabatic hypothesis applies to the processes $A^+ \rightarrow A^-$ and $A^0 \rightarrow A^-$. The only thing still unclear is the problem of the causes of the departure from exponential decrease of the cross sections σ_{1-1} and σ_{0-1} at the very smallest particle velocities studied in the present work. Regarding this there are three possible hypotheses: 1) the potential curves of the initial and final states of the system of colliding particles approach each other closely; 2) the constant a depends on the velocity of the particle; and 3) the relative velocity of the particles at which a process occurs is not equal to their relative velocity before the collision.*

The first hypothesis can be rejected at once, since it is contradicted by the small values of the cross sections in the region where the formula (1) is violated. Besides this, from the point of view of this hypothesis it cannot be understood why Eq. (1) holds in the region of higher velocities.

The departure of the points from the straight-line part of the graph of $\ln\sigma = f(1/v)$ is such that the second hypothesis can ascribe it to a decrease of the quantity a with decreasing velocity. For example, it is easily calculated that the deviation from the straight line shown by the last point on the graph of $\ln\sigma_{1-1} = f(1/v)$ for the process $Na^+ \rightarrow Na^-$ in H_2 corresponds to a decrease of a by 10 percent. It is improbable, however, that there is a decrease of a with decreasing velocity. It would rather be expected that a might decrease with increasing velocity.

To explain the violation of the formula (1) on the basis of the third hypothesis it is necessary to assume that $v_{true} > v$, where v_{true} is the velocity at which the process under consideration actually occurs, and v is the velocity before the collision. The increase of velocity $\Delta v = v_{true} - v$ is caused by the forces of interaction between the colliding particles. This increase of velocity can be caused by the forces that lead to the occurrence of the given process, but may be due to the action of other forces.

From elementary calculations we get the formula

$$\frac{\Delta p_{\parallel}}{p_{\parallel}} = \frac{v\left|\Delta\frac{1}{v}\right|}{1 - v\left|\Delta\frac{1}{v}\right|}, \qquad (27)$$

which enables us to compute the fractional change of the momentum component parallel to the path of the particle from the values of the experimentally determined quantities v and $|\Delta(1/v)|$. For example, for the three deviating points in Fig. 15 (velocities 4.1×10^7, 3.5×10^7 and 2.9×10^7 cm/sec) the quantity $\Delta p_{\parallel}/p_{\parallel}$ depends on the natures of the striking particle and the struck particle.

It must be emphasized that a rigorous proof of the correctness of the third hypothesis is a matter of great importance, since if this hypothesis is correct the departure of the points from the straight-line part of the graph of $\ln\sigma = f(1/v)$ can be used to calculate

*This last hypothesis was suggested by V. M. Dukel'skiĭ during a discussion at the Conference on Electronic and Atomic Collisions (Riga, June 1959).

the quantity $\Delta p_{\parallel}/p_{\parallel}$, which is not accessible to direct measurement.* So far, however, no other method for this proof can be seen than to make a direct calculation of the quantity $\Delta p_{\parallel}/p_{\parallel}$ and compare the calculated value with the value obtained from Eq. (27). The experimental information is still extremely inadequate for such comparisons, and therefore a very important task of the physics of atomic collisions is the further study of the functions $\sigma(v)$ for various processes in the low-velocity region.

This region is also interesting because for colliding particles with small numbers of electrons it is possible to make a quantum-mechanical calculation of the cross section of a process by using the method of perturbed stationary states.[52] Among the processes $A^+ \rightarrow A^-$ and $A^0 \rightarrow A^-$ considered here such a calculation has so far been made only for the process $H^+ \rightarrow H^-$ in He.[53] A comparison of the results of the theoretical calculation with the experimental data is shown in Fig. 18. As can be seen from this diagram, there is a large discrepancy between the experimental and theoretical results.

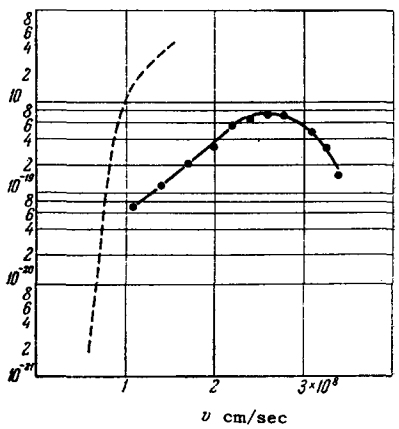

FIG. 18. The process $H^+ \rightarrow H^-$ in He; ——, experimental curve of $\sigma_{1\text{-}1}(v)$; – – –, curve constructed from the results of the theoretical calculation (ordinates are values of the cross section $\sigma_{1\text{-}1}$ in cm^2).

This discrepancy must evidently be explained by inexactness of the theoretical calculation, owing to the representation of the relative motion of the colliding particles in terms of plane waves; this is illegitimate for the region of slow collisions, which is the only type of collisions to which the method of perturbed stationary states can be applied. Future work of great interest is to make new and more accurate calculations for the processes $H^+ \rightarrow H^-$ and $H^0 \rightarrow H^-$ in He and H_2, and on the other hand to measure the effective cross sections of these processes at velocities lower than those studied so far.

d) Behavior of the Curve of $\sigma(v)$ in the Velocity Region $v > v_{max}$

The overwhelming majority of the curves of $\sigma(v)$ that have been obtained are located in the velocity region $v \leq v_{max}$. In this region there fall parts of the curves $\sigma_{1\text{-}1}(v)$ for the processes $H^+ \rightarrow H^-$ in He and H_2 and $Li^+ \rightarrow Li^-$ in H_2, and for the process $H^0 \rightarrow H^-$ in the five noble gases. The curves of $\sigma_{1\text{-}1}(v)$ are for cases in which the two-electron charge-transfer did not involve particles in excited states; that is, we are dealing with a "pure" $\sigma(v)$ curve. As for the process $H^0 \rightarrow H^-$ in inert gases, the branches of the curves of $\sigma_{0\text{-}1}(v)$ that are in the region $v > v_{max}$ can be distorted because of processes $H^0 \rightarrow H^-$ that occur with the production of a slow excited ion.

The possibility of such distortion depends on how close to the main maximum the additional maximum lies that is due to processes of electron capture accompanied by the production of a slow ion in the lowest excited state. Calculations show that for the process $H^0 \rightarrow H^-$ in He and Ne the additional maxima are located very far from the main maxima, so that in these cases the shape of the curves of $\sigma_{0\text{-}1}(v)$ is not distorted. In the cases of Ar, Kr, and Xe such distortion is quite possible, but owing to the much smaller probability of the process $H^0 + B \rightarrow H^- + B^{+}*$ as compared with the process $H^0 + B \rightarrow H^- + B^+$ it does not appreciably affect the shape of the curves of $\sigma_{0\text{-}1}(v)$ (see earlier argument).

It is interesting to find out how the behavior of the curve of $\sigma(v)$ in the region $v > v_{max}$ is affected by the type of process and the nature of the particles involved. For this purpose curves of the relation $\sigma/\sigma_{max} = f(v/v_{max})$ were constructed (Fig. 19) for the processes $H^+ \rightarrow H^-$ in He and H_2, $Li^+ \rightarrow Li^+$ in H_2, $H^0 \rightarrow H^-$ in He, and $H^+ \rightarrow H$ in He.† It must be pointed out that for the process $H^+ \rightarrow H$ in He the additional maxima associated with the production of excited ions in the process are far from the main maximum, so that also for this process we can assume that the shape of the curve of $\sigma_{10}(v)$ is undistorted in the range of velocities in question.

An examination of Fig. 19 leads to the following conclusions:

1) The decrease of the cross section with increasing velocity in the region $v > v_{max}$ is much more rapid for processes of two-electron charge transfer than for processes of one-electron charge transfer.

2) For two-electron charge transfer the behavior of the curve $\sigma/\sigma_{max} = f(v/v_{max})$ in the region $v > v_{max}$ depends neither on the nature of the ion nor on that of the gas.

3) In the region $v < v_{max}$ the behavior of all the curves is about the same.

The last of these deductions from the data leads to a certain conclusion regarding the constants k and σ_0 that appear in Eq. (1). On the basis of Eqs. (1) and (2) we can express the ratio σ/σ_{max} as a function of v/v_{max} in the form:

*Experiments on the scattering can give only $\Delta p_{\perp}/p_{\perp}$, i.e., the fractional change of the component of momentum perpendicular to the path of the particle.

†The data for the process $H^+ \rightarrow H$ in He are taken from reference 14.

$$\frac{\sigma}{\sigma_{max}} = \frac{\sigma_0}{\sigma_{max}} e^{-\frac{k}{v/v_{max}}}. \quad (28)$$

The identity of the behaviors of the curves of $\sigma/\sigma_{max} = f(v/v_{max})$ in the region $v < v_{max}$ leads to the conclusion that the quantities k and σ_0/σ_{max} are approximately the same for all the processes represented in Fig. 19. The physical meaning of the constancy of these quantities for such different processes is as yet unclear.

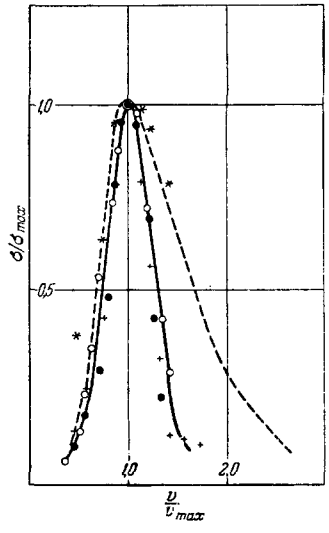

FIG. 19. Processes: – – – $H^+ \rightarrow H$ in He; * – $H^0 \rightarrow H^-$ in He; ● – $H^+ \rightarrow H^-$ in H_2; + – $H^+ \rightarrow H^-$ in He; o – $Li^+ \rightarrow Li^-$ in H_2.

e) Dependence of the Maximum Cross Section on Various Factors

Process $A^+ \rightarrow A^-$

One of the important quantities characterizing a curve $\sigma(v)$ is the quantity σ_{max}, i. e., the value of the cross section at its maximum. It is interesting to ascertain what factors affect this quantity. The quantity σ_{max} can naturally depend first of all on the nature of the interacting particles. An analysis of the experimental data on $A^+ \rightarrow A^-$ processes confirms this supposition. The quantity σ_{1-1max} depends both on the nature of the fast ion and on that of the target atom. The dependence on the nature of the fast ion is very strong, as can be seen from Fig. 20, which shows the curves of $\sigma_{1-1}(v)$ for seven ions (the target gas is Xe). The quantity σ_{1-1max} varies over a very wide range, from 5×10^{-19} cm^2 (Li^+) to 2×10^{-16} cm^2 (O^+).

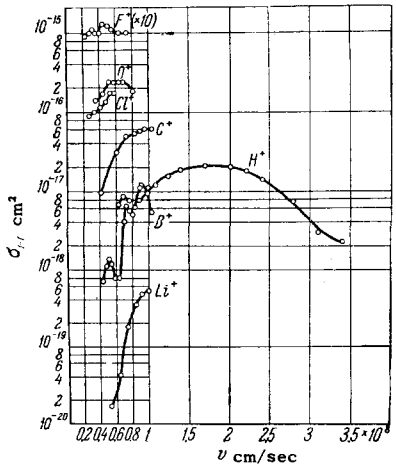

FIG. 20. Curves of $\sigma_{1-1}(v)$ for processes $A^+ \rightarrow A^-$ in Xe.

When the result of the process $A^+ \rightarrow A^-$ is the production of a negative ion in the ground state the capture of the two electrons occurs to two levels whose binding energies are the first ionization potential of the atom A and its electron affinity. We can make the hypothesis that the effect of the nature of the ion on the quantity σ_{1-1max} is connected with the values of the binding energies of the levels of the atom A to which the electrons are captured. From the point of view of this hypothesis it would be reasonable to expect that the quantity σ_{1-1max} increases monotonically with increase of the sum $V_A^I + S_A$, or, since $V_A^I \gg S_A$, with increase of V_A^I. Figure 21 shows curves of the dependences of σ_{1-1max} on the quantities V_A^I, S_A, and $V_A^I + S_A$, which show that there is no monotonic relation between σ_{1-1max} and either V_A^I or the sum $V_A^I + S_A$. It follows from this that the binding energies of the levels to which the electrons are captured do not completely determine the values of σ_{1-1max}, although they undoubtedly have an important effect on this quantity. This can at any rate be seen from the fact that the most abrupt violation of the monotonic character of the curves of $\sigma_{1-1max} = f(V_A^I)$ and $\sigma_{1-1max} = f(V_A^I + S_A)$ is given by the ion H^+. This is evidently due to the fact that the H atom has about the same value for the first ionization potential as the O and Cl atoms, but a much smaller value of the electron affinity than those atoms, which leads to a decrease of the value of σ_{1-1max} for the process $H^+ \rightarrow H^-$ as compared with the processes $O^+ \rightarrow O^-$ and $Cl^+ \rightarrow Cl^-$. On the other hand, it can be seen from a comparison of the values of σ_{1-1max} for the processes $H^+ \rightarrow H^-$, $B^+ \rightarrow B^-$ and $Li^+ \rightarrow Li^-$ that energetic parameters alone are insufficient for the determination of the quantity σ_{1-1max}. In fact, the values of the electron affinity for the atoms H, B, and Li are about the same, and the ionization potentials are 13.54, 8.28, and 5.37 ev, respectively. But the decrease of the ionization potential as we go from the H atom to the B atom does not lead to a decrease of σ_{1-1max}, whereas as we go on to the Li atom the decrease of the ionization potential leads to a large decrease of σ_{1-1max}. It is possible that in this case there is an effect of the difference between the

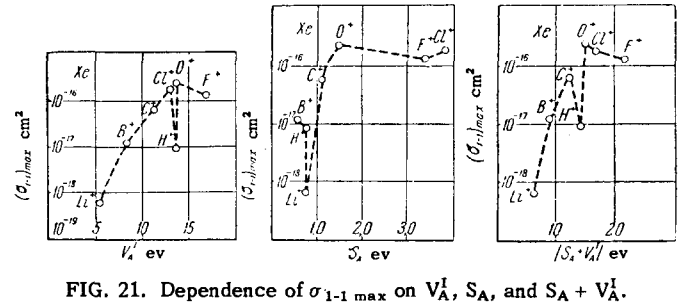

FIG. 21. Dependence of $\sigma_{1-1\ max}$ on V_A^I, S_A, and $S_A + V_A^I$.

electronic configurations of the initial and final states of the particle that captures the two electrons. The processes $H^+ \rightarrow H^-$ and $Li^+ \rightarrow Li^-$ accomplish the filling of the 1s and 2s shells, whereas the process $B^+ \rightarrow B^-$ begins the filling of the 2p shell. Evidently the electronic configuration of the fast ion has a definite significance. In cases in which the electron shell of the ion is closed, the quantity $\sigma_{1-1\max}$ is very small (the ions Li^+, K^+, B^+). For the ion H^+, however, which is a bare nucleus, one gets a relatively small value of $\sigma_{1-1\max}$. Thus the available experimental material allows us to conclude that the quantity $\sigma_{1-1\max}$ is affected both by the binding energies of the levels to which the electrons are captured and by the electron shell structure of the fast ion.

A more definite conclusion can be reached regarding the effect of the nature of the target atom on the quantity $\sigma_{1-1\max}$. The typical variation of the curves of $\sigma_{1-1}(v)$ as we go from one target atom to another is illustrated in Fig. 22, which shows these curves for the process $O^+ \rightarrow O^-$ in Ne, Ar, Kr, and Xe. It can be seen that the effect of the nature of the target atom on the curve of $\sigma_{1-1}(v)$ shows itself in two ways: 1) with increase of the atomic number of the target gas the maximum is displaced in the direction of smaller velocities, as was to be expected, since the position of the maximum on a curve of $\sigma_{1-1}(v)$ is determined by the Massey adiabatic criterion; 2) the value of the cross section at the maximum increases with increasing atomic number of the target gas. It is useful to relate the dependence of $\sigma_{1-1\max}$ on the nature of the target atom to the binding energy of the electrons torn off from the target atom, i. e., with the sum $V_B^I + V_B^{II}$ of the first and second ionization potentials of this atom. The dependence of $\sigma_{1-1\max}$ on $V_B^I + V_B^{II}$ is shown in Fig. 23. An examination of this diagram yields the conclusion that the quantity $\sigma_{1-1\max}$ decreases monotonically with increase of the binding energy of the electrons removed from the target atom.

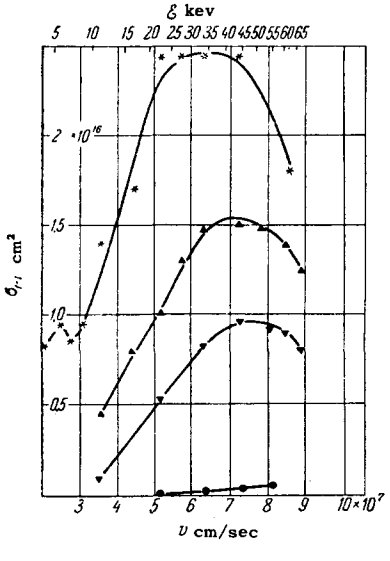

FIG. 22. Process $O^+ \rightarrow O^-$; * – Xe; ▲ – Kr; ▼ – Ar; ● – Ne.

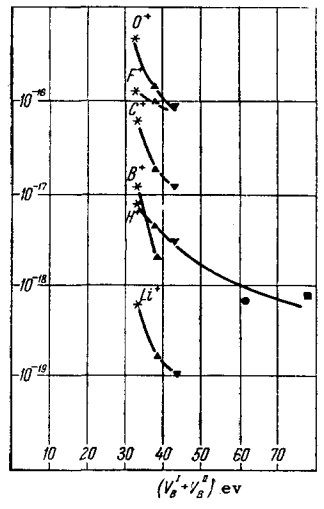

FIG. 23. * – Xe; ▲ – Kr; ▼ – Ar; ● – Ne; ■ – He.

In reference 54 it is shown that there is a definite dependence of the maximum value of the cross section of the process $A^+ \rightarrow A$ (one-electron charge transfer) on the resonance defect. As can be seen from Fig. 24, which shows the dependence of $\sigma_{1-1\max}$ on $|\Delta E|$, the resonance defect is not a universal parameter that determines the value of $\sigma_{1-1\max}$, since the points of the plot of $\sigma_{1-1\max} = f(|\Delta E|)$ lie on different curves for different ions, which reflects a a dependence of $\sigma_{1-1\max}$ on the nature of the fast ion. For all ions there is a monotonic decrease of $\sigma_{1-1\max}$ with increase of the absolute value of the resonance defect. The points for molecular gases depart from this monotonic dependence.

Process $A^0 \rightarrow A^-$

The quantity $\sigma_{0-1\max}$ also depends strongly on the nature of the fast particle, as can be seen from Fig. 25, which shows the curves of $\sigma_{0-1}(v)$ for six atoms in Xe. In this case the effect of the binding energy of the level into which the electron is captured can be characterized by the quantity S_A. The dependence of $\sigma_{0-1\max}$ on S_A for collisions in Kr and Xe is shown in Fig. 26. In the sequence of fast atoms from He to O there is a monotonic increase of $\sigma_{0-1\max}$ with increasing S_A, but the further increase of S_A

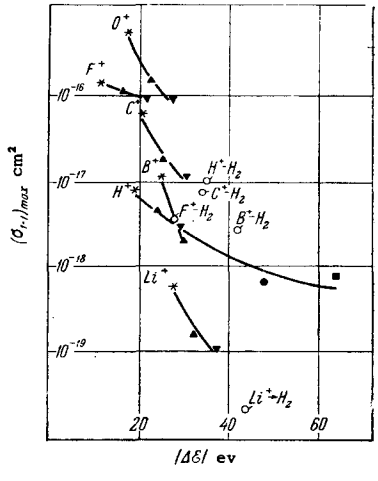

FIG. 24. * – Xe; ▲ – Kr; ▼ – Ar; ● – Ne; ■ – He; o – H_2.

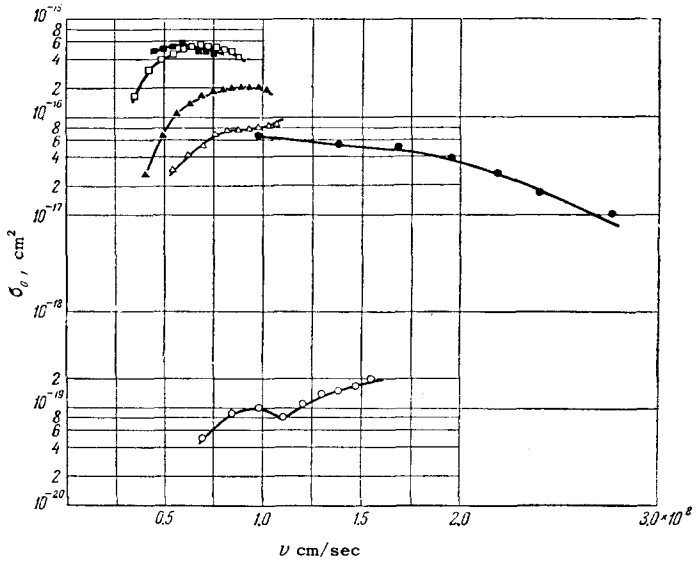

FIG. 25. Curves of $\sigma_{1\text{-}1}(v)$ for process $A^0 \rightarrow A^-$ in Xe: ○ – He; ● – H; ▲ – C; □ – O; ■ – F; △ – B.

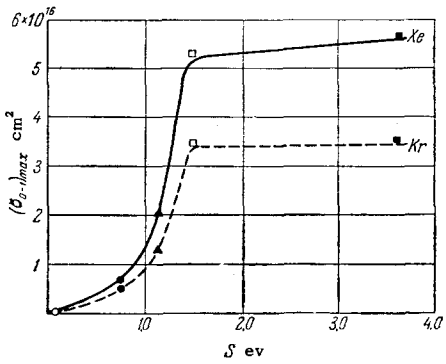

FIG. 26. ○ – He; ● – H; ▲ – C; □ – O; ■ – F.

as we go from O to F does not lead to any marked increase of $\sigma_{0\text{-}1\,max}$. A similar behavior is also found for the quantity $\sigma_{1\text{-}1\,max}$ (see Fig. 21).

The effect of the nature of the target atom on the curve of $\sigma_{0\text{-}1}(v)$ is the same as in the case of two-electron charge transfer, as can be seen from Fig. 27, which shows the curves for the process $O^0 \rightarrow O^-$ in five noble gases. Just as in the case of the process $A^+ \rightarrow A^-$, there is a decrease of $\sigma_{0\text{-}1\,max}$ with increase of the binding energy of the electron torn off from the target atom, as can be seen from Fig. 28, which shows a plot of $\sigma_{0\text{-}1\,max} = f(V_B^I)$. The lack of a monotonic dependence of $\sigma_{0\text{-}1\,max}$ on V_B^I for He atoms is due to the presence of metastable He atoms in the primary beam. Also in the case of the process $A^0 \rightarrow A^-$ the resonance defect is not a universal parameter that determines the value of $\sigma_{0\text{-}1\,max}$, as one sees on constructing a plot of $\sigma_{0\text{-}1\,max} = f(|\Delta E|)$.

f) Comparison of the Cross Sections of the Processes $A^+ \rightarrow A^0$, $A^0 \rightarrow A^-$, and $A^+ \rightarrow A^-$

In all cases in which there are experimental data for the processes $A^+ \rightarrow A^0$, $A^0 \rightarrow A^-$, and $A^+ \rightarrow A^-$

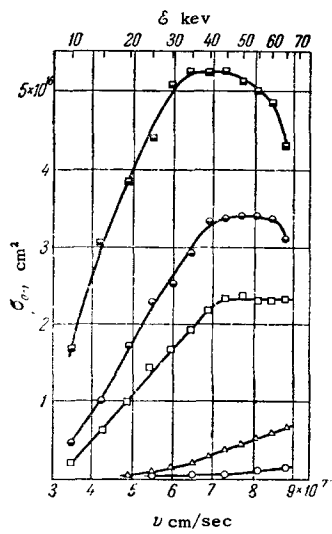

FIG. 27. Process $O^0 \rightarrow O^-$; ○ – He; △ – Ne; □ – Ar; ⊖ – Kr; ■ – Xe.

that allow us to compare the cross sections σ_{10}, $\sigma_{0\text{-}1}$, and $\sigma_{1\text{-}1}$, it is found that $\sigma_{10} > \sigma_{0\text{-}1} > \sigma_{1\text{-}1}$. An idea of the differences in the values of these cross sections is given by Fig. 29,* which shows graphs of $\sigma_{10}(v)$, $\sigma_{0\text{-}1}(v)$, and $\sigma_{1\text{-}1}(v)$ for the combinations C – Xe, H – Xe, H – He, and H – Ar. It can be seen that the cross section σ_{10} is larger than $\sigma_{1\text{-}1}$ by about two orders of magnitude, while $\sigma_{0\text{-}1}$ is several times as large as $\sigma_{1\text{-}1}$. The differences between the values of the cross sections σ_{10}, $\sigma_{0\text{-}1}$, and $\sigma_{1\text{-}1}$ are due, on one hand, to the different numbers of electrons that are captured, and, on the other hand, to the different binding energies of the levels into which the electrons are captured. The very large difference between the cross sections σ_{10} and $\sigma_{1\text{-}1}$ reflects the difference between the probabilities of one-electron and two-electron processes. The almost equally large difference between the cross sections σ_{10} and $\sigma_{0\text{-}1}$ is due to the fact that these cross sections give the probabilities of capture of an electron to levels with decidedly different binding energies. The comparatively small difference between the cross sections of the one-electron process $A^0 \rightarrow A^-$ and the two-electron process $A^+ \rightarrow A^-$ is due to the fact that in the former case the capture of the electron is to a level with a small bind-

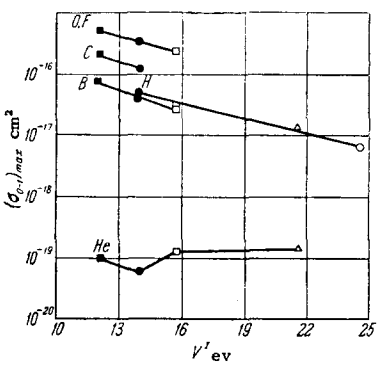

FIG. 28. ■ – Xe; ● – Kr; □ – Ar; △ – Ne; ○ – He; (abscissa is value of V_B^I).

*The values of the cross sections σ_{10} are taken from references 14 and 16.

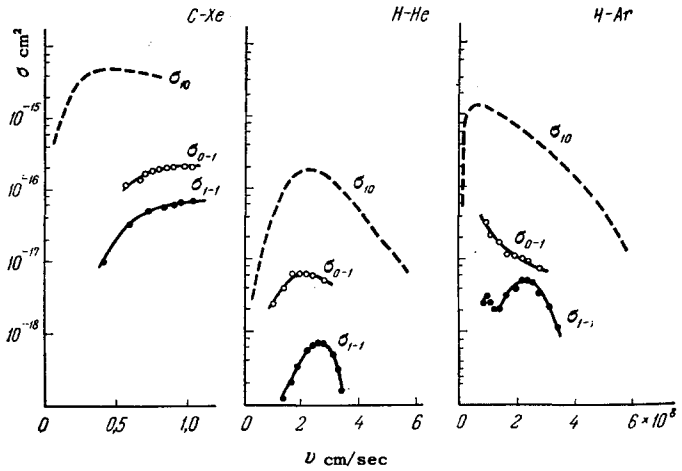

FIG. 29

ing energy, and in the latter case one of the levels to which the electrons are captured has a large binding energy.

g) The Production of Slow Negative Ions in Atomic Collisions

As was shown in the introduction, slow negative ions are produced as the result of processes (IIa) and (IIb) when fast negative and positive ions pass through gases.

The effective cross sections for processes of production of slow negative ions are measured by collecting the ions on a measuring electrode. The particulars of this method are described in references 23, 55, and 56. To separate the slow negative ions from the electrons that are produced by stripping of fast ions and ionization of particles of the gas, the measuring condenser is placed in a magnetic field with the field parallel to the plates of the condenser.

The first measurements of the cross sections for production of slow negative ions in the passage of the ions Na^-, K^-, O^-, Cl^-, OH^-, and O_2^- at energy 720 ev through oxygen were made in reference 57. For ions of such low energy it may be assumed that the cross section for charge transfer from the negative ions [process (IIA)] is much larger than that for dissociation of O_2 molecules into negative and positive ions, so that we may suppose that the cross sections measured by those authors give the probabilities for charge transfer from the negative ions in oxygen. The results of the measurements are given in Table VII.*

As can be seen from Table VII, the charge-transfer cross sections for some ions are very large. The possibility is not excluded that the energy of the ion for which the cross section has been measured is in the neighborhood of the maximum of the curve of σ_{trans} $\sigma_{trans}(E)$. There is a marked dependence of the cross section on the resonance defect. Just as for charge transfer from positive ions, the cross section increases with decrease of the resonance defect.

TABLE VII

Ion	Charge-transfer cross section in cm^2	Resonance defect ΔE in ev
Na^-	$5 \cdot 0^{-15}$	−0.65
K^-	$6 \cdot 10^{-15}$	−0.65
O^-	$5 \cdot 10^{-16}$	−1.3
Cl^-	$3 \cdot 10^{-17}$	−3.7
OH^-	$6 \cdot 10^{-18}$	−2.0
O_2^-	$2 \cdot 10^{-15}$	0

The authors compared the cross sections for the resonance processes $O_2^- + O_2 \rightarrow O_2 + O_2^-$ and $O_2^+ + O_2 \rightarrow O_2 + O_2^+$ at the same energy of the ions. It was found that the charge-transfer cross section for the O_2^+ ion is considerably larger (5×10^{-15} cm^2) than the corresponding quantity for O_2^-. Thus the rule found for positive ions, that the cross section for resonance charge transfer increases in inverse proportion to the ionization potential of the atom evidently does not extend to the case of negative ions. The larger charge-transfer cross section of the O_2^+ ion as compared with that of the O_2^- ion is explained by the authors of reference 57 by the fact that in the case of the positive ion the electron that makes the transition is in the long-range field of the positive ion; the transition of the excess electron of a negative ion occurs in the short-range field of the neutral atom.

Reference 61 reports measurements of the cross section σ_u^- for production of slow negative ions in the passage of H^- and O^- ions with energies from 10 to 50 kev through O_2 and CCl_4. Since the ions of the primary beam had a rather large energy, slow negative ions could arise not only owing to charge transfer, but also owing to dissociation of molecules into positive and negative ions. The curves of $\sigma_u^-(v)$ for the ion-molecule combinations that were studied are shown in Fig 30. For comparison the diagram also shows

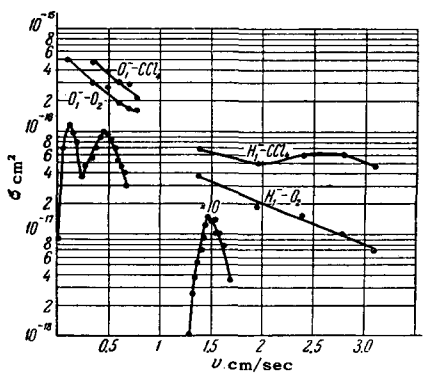

FIG. 30. The lower curves on the left and right are for the combinations e–CCl_4 and e – O_2, respectively. Abscissa times 10^8 is v in cm/sec.

*The resonance defects given in Table VII are calculated on the assumption that the ion O_2^- produced by charge transfer does not dissociate. The numerical values of ΔE differ from those given in reference 57, since in obtaining the values of ΔE given in Table VII new values were used for the electron affinities of O,[58] Na, and K[59] atoms and O_2 molecules.[60]

curves of $\sigma_u^-(v)$ for the production of negative ions in collisions of electrons with O_2 and CCl_4 molecules, taken from reference 62, and also one point for the combination $O^- - O_2$ from the data of reference 57 (cf. Table VII).

As can be seen from Fig. 30, the values of the cross section σ_u^- for the combination $H^- - O_2$ vary over the range $(1 \text{ to } 3) \times 10^{-17}$ cm^2, and the values are an order of magnitude larger for the combination $O_1^- - O_2$. In reference 63 estimates have been made of the cross section for dissociation of an O_2 molecule into positive and negative ions by the impacts of protons with energies from 10 to 30 kev. These cross sections turned out to be of the order of 10^{-19} cm^2. Since it is improbable that the cross section for dissociation of O_2 by impacts of H^- ions would be much larger than the corresponding cross section for H^+ ions, it must be supposed that the cross sections σ_u^- for the combinations $H^- - O_2$ and $O^- - O_2$ are the cross sections for charge transfer from the H^- and O^- ions in oxygen.

The increase of σ_u^- with decrease of the velocity of the ion indicates that the maxima of the curves of $\sigma_u^-(v)$ for the combinations $H^- - O_2$ and $O^- - O_2$ are located at small velocities. This was indeed to be expected on the basis of the adiabatic criterion, since the resonance defects of the processes of charge transfer from H^- and O^- ions in oxygen are small. As for the maxima of the curves of $\sigma_u^-(v)$ for the combinations $H^- - CCl_4$ and $O^- - CCl_4$, it can be seen from the behavior of these curves that these maxima are also located in the low-velocity region. The maximum at a velocity 2.6×10^8 cm/sec on the curve of $\sigma_u^-(v)$ for the combination $H^- - CCl_4$ is possibly due to charge transfer with subsequent dissociation of the unstable ion CCl_4^-.

A point that calls for attention is the large difference between the sizes of the cross sections σ_u^- and the shapes of the curves of $\sigma_u^-(v)$ for processes of adhesion of free electrons to molecules and for processes of charge transfer from negative ions to the same molecules. This difference is not surprising if we recall that in the former case the negative ion is formed by the uniting of a free electron with the molecule, whereas in the latter case the production of the negative ion is due to a transition of an electron between discrete states of the negative ion and the gas molecule.

The data that have been given on the production of slow negative ions in atomic collisions show that it is desirable to make further studies in the low-velocity region, where the maxima of the curves of $\sigma_u^-(v)$ are located. Determination of the positions of these maxima and the shapes of the curves of $\sigma_u^-(v)$ in the region $v < v_{max}$ will make it possible to settle the question of the applicability of the adiabatic hypothesis to processes of charge transfer from negative ions. Much information useful for the understanding of processes of charge transfer from negative ions can also be given by mass-spectrum analyses of slow negative ions produced by charge transfer.

CONCLUSION

The results of experimental studies of processes of production of fast and slow negative ions in atomic collisions that are given in the present article allow us to conclude that these studies have already made a considerable contribution to the physics of atomic collisions. It must be emphasized, however, that more extensive and deeper studies of the processes considered in this article are necessary. In particular, the study of the function $\sigma(v)$ in the adiabatic region right down to the threshold of the process is of great interest for the theory of atomic collisions. It is desirable in future to study the scattering and energy loss in processes of formation of negative ions. There is also some interest in the study of these processes in the region of higher velocities, where in some cases they can be treated theoretically by means of the Born approximation.

[1] H. S. W. Massey, Negative Ions, London, 1950, Camb. U. Press.

[2] H. Neuert, Ergebn. exakt. Naturwiss. **29**, 1-60 (1956).

[3] F. H. Field and J. L. Franklin, Electron Impact Phenomena and the Properties of Gaseous Ions, New York, 1957, Academic Press.

[4] N. S. Buchel'nikova, Usp. Fiz. Nauk **65**, 351 (1958).

[5] É. Ya. Zandberg and N. I. Ionov, Usp. Fiz. Nauk **67**, 581 (1959), Soviet Phys. Uspekhi **2**, 255 (1959).

[6] E. B. Armstrong and A. Dalgarno, The Airglow and the Aurorae, p. 328, London, 1955.

[7] L. D. Landau, Physik. Z. Sowjetunion **1**, 88 (1932).

[8] C. Zener, Proc. Roy. Soc. **A137**, 696 (1932).

[9] E. C. G. Stueckelberg, Helv. Phys. Acta **5**, 369

[10] H. S. W. Massey, Rept. Progr. Phys. **12**, 248 (1948).

[11] G. F. Drukarev, JETP **37**, 847 (1959), Soviet Phys. JETP **10**, 603 (1960).

[12] J. B. Hasted, Proc. Roy. Soc. **A205**, 421 (1951).

[13] J. B. Hasted, Proc. Roy. Soc. **A212**, 235 (1952).

[14] J. B. H. Stedeford and J. B. Hasted, Proc. Roy. Soc. **A227**, 466 (1955).

[15] J. B. Hasted and R. A. Smith, Proc. Roy. Soc. **A235**, 354 (1956).

[16] H. B. Gilbody and J. B. Hasted, Proc. Roy. Soc. **A238**, 334 (1957).

[17] J. B. Hasted, J. Appl. Phys. **30**, 25 (1959).

[18] D. R. Bates and H. S. W. Massey, Philos. Mag. **45**, 111 (1954).

[19] L. W. Alvarez, Rev. Scient. Instrum. **22**, 708 (1951).

[20] W. Wien, Ann. Phys. **39**, 519 (1912).

[21] S. K. Allison, Rev. Mod. Phys. **30**, 1137 (1958).

[22] Leviant, Korsunskiĭ, Pivovar, and Podgornyĭ, Dokl. Akad. Nauk SSSR **103**, 403 (1955).

[23] Fogel', Krupnik, and Safronov, JETP 28, 589 (1955), Soviet Phys. JETP 1, 415 (1955).
[24] Ya. M. Fogel' and L. I. Krupnik, JETP 29, 209 (1955), Soviet Phys. JETP 2, 252 (1956).
[25] Ya. M. Fogel' and R. V. Mitin, JETP 30, 450 (1956), Soviet Phys. JETP 3, 324 (1956).
[26] Fogel', Mitin, and Koval', JETP 31, 397 (1956), Soviet Phys. JETP 4, 359 (1957).
[27] Fogel', Ankudinov, Pilipenko, and Topolya, JETP 34, 579 (1958), Soviet Phys. JETP 7, 400 (1958).
[28] Fogel', Mitin, and Kozlov, J. Tech. Phys. (U.S.S.R.) 28, 1526 (1958), Soviet Phys.-Tech. Phys. 3, 1410 (1959).
[29] N. V. Fedorenko, J. Tech. Phys. (U.S.S.R.) 24, 769 (1954).
[30] V. M. Dudel'skiĭ and N. V. Fedorenko, JETP 29, 473 (1955), Soviet Phys. JETP 2, 307 (1956).
[31] Fogel', Lisochkin, and Stepanova J. Tech. Phys. (U.S.S.R.) 25, 1944 (1955).
[32] Fogel', Krupnik, and Ankudinov, J. Tech. Phys. (U.S.S.R.) 26, 1208 (1956), Soviet Phys.-Tech. Phys. 1, 1181 (1957).
[33] Fogel', Krupnik, Koval', and Slabospitskii, J. Tech. Phys. (U.S.S.R.) 27, 988 (1957), Soviet Phys.-Tech. Phys. 2, 902 (1957).
[34] Ya. M. Fogel' and A. D. Timofeev, Тр. физ.-мат. фак-та ХГУ (Trans. Phys.-Math. Fac. Khar'kov State University) 7, 177 (1958).
[35] V. L. Tal'roze and E. L. Frankevich, Dokl. Akad. Nauk SSSR 111, 376 (1956).
[36] N. V. Fedorenko, J. Tech. Phys. (U.S.S.R.) 24, 784 (1954).
[37] Ya. M. Fogel' and R. V. Mitin, loc. cit. ref. 34, 7, 195 (1958).
[38] Fogel', Mitin, Kozlov, and Romashko, JETP 35, 565 (1958), Soviet Phys. JETP 8, 390 (1959).
[39] Fogel', Kozlov, Kalmykov, and Muratov, JETP 36, 1312 (1959), Soviet Phys. JETP 9, 929 (1959).
[40] Fogel', Kozlov and Kalmykov, JETP 36, 1354 (1959), Soviet Phys. JETP 9, 963 (1950).
[41] Fogel', Kozlov, and Polyakova, JETP (in press).
[42] Fogel', Ankudinov, and Pilipenko, JETP 35, 868 (1958), Soviet Phys. JETP 8, 600 (1959).
[43] Fogel', Ankudinov, and Pilipenko, JETP 38, 26 (1960), Soviet Phys. JETP 11, 18 (1960).
[44] Dukel'skii, Afrosimov, and Fedorenko, JETP 30, 792 (1956), Soviet Phys. JETP 3, 764 (1956).
[45] Fedorenko, Afrosimov, and Kaminker, J. Tech. Phys. (U.S.S.R.) 26, 1929 (1956), Soviet Phys.-Tech. Phys. 1, 1861 (1957).
[46] C. E. Moore, Atomic Energy Levels, Circular 467, National Bureau of Standards, 1949.
[47] O. Henle and W. Maurer, Physik. Z. 37, 659 (1936).
[48] W. de Groot and F. M. Penning, Handbuch der Physik 23, 23 (1933).
[49] H. D. Hagstrum and J. T. Tate, Phys. Rev. 59, 354 (1941).
[50] W. Maurer, Physik. Z. 40, 161 (1939).
[51] O. Beeck, Physik. Z. 35, 36 (1934).
[52] H. S. W. Massey and R. A. Smith, Proc. Roy. Soc. A142, 142 (1933).
[53] L. N. Rozentsveĭg and V. I. Gerasimenko, loc. cit. ref. 34, 6, 87 (1955).
[54] N. V. Fedorenko and V. A. Belyaev, JETP 37, 1808 (1959), Soviet Phys. JETP 10, 1276 (1960).
[55] J. P. Keene, Philos. Mag. 40, 369 (1949).
[56] N. V. Fedorenko, J. Tech. Phys. (U.S.S.R.) 24, 2113 (1954).
[57] V. M. Dukel'skiĭ and É. Ya. Zandberg, Dokl. Akad. Nauk SSSR 82, 33 (1952).
[58] L. M. Branscomb and S. J. Smith, Phys. Rev. 98, 1127 (1955).
[59] B. Gáspár and B. Molnár, Acta, phys. Hungar. 5, 75 (1955).
[60] Burch, Smith, and Branscomb, Phys. Rev. 112, 171 (1958).
[61] Fogel', Koval', and Levchenko, JETP (in press).
[62] N. S. Buchel'nikova, JETP 35, 1119 (1958), Soviet Phys. JETP 8, 783 (1959).
[63] Il'in, Afrosimov, and Fedorenko, JETP 36, 41 (1959), Soviet Phys. JETP 9, 29 (1959).

Translated by W. H. Furry